Research Square

Preprints are preliminary reports that have not undergone peer review.
They should not be considered conclusive, used to inform clinical practice,
or referenced by the media as validated information.

Transient overexpression and silencing of tomato SlGLP11-1 gene reveal its crucial role in mediating ROS homeostasis driven disease resistance

Pooja Prajapati
Savitribai Phule Pune University
Tushar Khobragade
Savitribai Phule Pune University
Avinash Kamble
ackamble@unipune.ac.in

Savitribai Phule Pune University

Research Article

Keywords: genome wide, silencing, overexpression, hydrogen peroxide, Botrytis, Fusarium, resistance

Posted Date: October 30th, 2026

DOI: https://doi.org/10.21203/rs.3.rs-11217426/v1

License: This work is licensed under a Creative Commons Attribution 4.0 International License.
Read Full License

Additional Declarations: No competing interests reported.

Transient overexpression and silencing of tomato *SlGLP11-1* gene reveal its crucial role in mediating ROS homeostasis driven disease resistance

Main Conclusion:

Tomato *SlGLP11*-1 positively regulates defence against *Botrytis cinerea* by promoting H_2O_2 accumulation, highlighting its potential role in ROS-mediated immunity in tomato.

Abstract:

Germin and germin- like proteins (GLPs) are known to play various roles in plant development and in response to biotic and abiotic stress. Many GLPs have been reported to show differential expression in response to pathogen infections, indicating their direct roles in host- pathogen interactions. Despite their significant roles in plant immunity, the tomato (*Solanum lycopersicum* L.) GLP members have not been studied comprehensively at the genome- wide scale. Also, very few reports exist on the functions and activities of tomato GLP gene family members. In this study, GLP family members in tomato were analysed and a standardised nomenclature for tomato GLP genes was defined. The chromosomal distribution of GLP genes in tomato was determined, and a phylogenetic analysis was performed. In addition, the in silico subcellular localization of GLPs in tomato was predicted, and gene expression was examined in response to different phytohormone treatments and pathogen infection. Finally, we identified candidate pathogen- responsive *SlGLPs* and functionally characterized *SlGLP11-1*. Transient overexpression of *SlGLP11-1* in *Nicotiana* leaves enhanced resistance against *Botrytis cinerea*. Similarly transient silencing of *SlGLP11-1* by virus induced gene silencing (VIGS) in tomato leaves increased susceptibility to *Botrytis cinerea* infection. We also, estimated endogenous H_2O_2 levels and catalase activity in the transient *SlGLP11*-1 overexpressed and silenced leaves of *Nicotiana benthamiana* and tomato respectively, all with and without Botrytis infection. Our results establish that *SlGLP11*-1 functions as a positive regulator of ROS-mediated plant defence by promoting H_2O_2 accumulation during both basal and pathogen challenged conditions, with catalase activity tracking H_2O_2 levels as a secondary antioxidant response. This study will serve as a foundation for future functional investigations of tomato GLP family members playing role in the plant immunity.

Key words: genome wide, silencing, overexpression, hydrogen peroxide, *Botrytis*, *Fusarium*, resistance

Introduction

Germin and germin-like proteins (GLPs) were first discovered as germination markers in wheat seeds (Lane 2002; Dunwell et al. 2008), and were later reported in monocotyledons, dicotyledons, and gymnosperms (Dunwell et al. 2008). These were further characterized as homohexamer glycoprotein, some of which exhibit oxalate oxidase (OXO, EC 1.2.3.4) activity. GLPs possess a conserved β-sheet barrel domain involved in metal binding and active site modification, enabling both enzymatic and non-enzymatic activities (Barman and Banerjee 2015). Most GLPs are stable oligomers, exhibiting enzyme activity in hexameric forms composed of trimers of dimers (Dunwell et al. 2008; Pei et al. 2020). The germin family belongs to the functionally diverse cupin superfamily; germin genes typically contain two exons and encode a conserved "cupin" domain (PF00190) at the C-terminus. Classification of germins and GLPs remains challenging because of their highly conserved sequences and structural similarities (Agarwal et al. 2009).

GLPs share sequence and structural similarities with wheat germin (Patnaik and Khurana, 2001). They form a heterogeneous group of soluble proteins and have a greater taxonomic coverage in plants, whereas "true germins" represent a well- conserved homogeneous group, found almost exclusively in cereal species (Bernier and Berna 2001; Kurtz 2001; Carrillo et al. 2009; Davidson et al. 2009). Enzymatic activity in most GLPs occurs only in polymeric forms, although one GLP from *Capsicum chinense* exhibits superoxide dismutase (SOD) activity without polymerization (Cheng et al. 2014; Mejía-Teniente et al. 2015; Sakamoto et al. 2015). Six germin proteins from barley form an extraordinarily stable hexameric protein structure by binding a single manganese ion (Kurtz 2001). In addition to OXO activity, GLPs have also been reported to putative function as auxin receptors, superoxide dismutase (SOD, EC 1.15.1.1), ADP glucose pyrophosphatase/phosphodiesterase (AGPPase, EC 3.1.4.1), polyphenol oxidase (PPO), and serine protease inhibitors (Rodríguez-López et al. 2001;

Segarra et al. 2003; Cheng et al. 2014; Beracochea et al. 2015; Huang et al. 2015; Sakamoto et al. 2015; Pei et al. 2020). GLP genes are expressed in various organs, including leaves, cotyledons, stems, roots, embryos, flowers, and seeds, and play roles in development (Wang et al. 2013; Li et al. 2016). In *Arabidopsis* and rice, overexpression of GLP genes altered normal plant growth and development (Banerjee and Maiti 2010; Ham et al. 2012). Furthermore, differential spatio-temporal expression of GLP genes in different plants potentially influences enzyme activity (Li et al. 2016). During germination, GLP genes are expressed in the apoplast and cell wall of embryonic cells, and they may contribute in cell defence (Bernier and Berna 2001).

Many GLP genes occur in multiple copies at specific chromosomal loci (Davidson et al. 2009). All germin and GLP polypeptides contain a putative signal peptide, and mature proteins feature three highly conserved oligopeptides (boxes A, B, and C) containing three histidine residues and one glutamate residue, conserved within GLP subfamilies (Bernier and Berna 2001). Based on sequence, biochemical activity and function, the GLP family is classified into two major groups. The first category, oxalate oxidases (OXO), is found in true cereals such as barley, wheat, and corn, and has fewer members. The second class of GLPs has more members than the first, with significant sequence variations between members (Lane 2002). Numerous studies have linked GLPs to defence and tolerance mechanisms (Govindan et al. 2024). GLP expression increases in response to pathogen infections, insect herbivory, or exposure to chemicals such as salicylic acid, hydrogen peroxide, or ethylene (Godfrey et al. 2007). High GLP expression is also induced by abiotic stresses including salinity, drought, heavy metals, and wounding (Bernier and Berna 2001; Houde and Diallo 2008; Wang et al. 2013). Furthermore, GLP genes respond to fungal, bacterial, and viral pathogens (Godfrey et al. 2007; Knecht et al. 2010; Rietz et al. 2012; Mejía-Teniente et al. 2015). Following infection, GLP expression often increases in cell walls, likely contributing to plant defence via reactive oxygen

species (ROS) generation and an oxidative burst (Godfrey et al. 2007; Averyanov 2009). Several studies have linked GLP gene clusters with disease resistance traits (Manosalva et al. 2009; Himmelbach et al. 2010).

Although the roles of many GLP genes remain unclear, functional analyses across multiple plant species highlight their importance in growth, development, and stress responses. In barley, wheat, soybean, and moss, GLP genes have been extensively characterized (Schweizer et al. 1999; Nakata et al. 2004; Zimmermann et al. 2006). In rice, *OsGLP1* (*Os08g35760*, also known as *OsGLP8-14*) is primarily expressed in green vegetative tissues and influences plant height (Banerjee and Maiti 2010). *OsGLP2-1* (*Os02g29000*) regulates seed dormancy through abscisic acid (ABA) and gibberellic acid (GA) signaling (Wang et al. 2020). Overexpression of *OsRGLP1* (*Os08g09080*, also known as *OsGLP8-11*) in tomato altered chlorophyll content, relative water content, plant stature, and trichome traits (Perveen et al. 2021). Multiple rice GLP genes respond to biotic stresses such as brown planthopper, *Agrobacterium tumefaciens*, and fungal pathogens, as well as abiotic stresses including cold, salinity, drought, and anoxia (Das et al. 2019). Overexpression of *OsRGLP1* enhanced SOD activity, enabling prediction of residues involved in metal ion and substrate binding (Shahwar et al. 2023). *OsGLP8-14* has been linked to disease resistance, salinity tolerance, and UV-B acclimation (Banerjee and Maiti 2010; He et al. 2021). GLPs also function in plant disease resistance. Transgenic tobacco plants overexpressing *Lilium regale LrGLP1* and *Medicago truncatula* overexpressing *OsRGLP1* exhibited enhanced resistance to *Fusarium oxysporum* infection (Zhang et al. 2017; Sultana et al. 2016). Raspberry GLP *RiABP19* has also been shown to regulate immunity in response to *Phytophthora* root rot (Osama et al. 2025).

Rice GLP gene *OsGLP2-4* (*Os02g32980*) imparts resistance to fungal blast and bacterial blight through jasmonic acid (JA)-dependent pathway (Liu et al. 2016). Cotton *GhABP19* is also linked to the JA-mediated defence response to infection by *Verticillium dahliae* and *Fusarium*

oxysporum (Pei et al. 2020). Overexpression of sunflower *HaGLP1* in *Arabidopsis* increased resistance to fungal infections by enhancing the accumulation of ROS (Beracochea et al. 2015). Resistance to *Sclerotinia sclerotiorum* infection was increased in transgenic tobacco plants overexpressing the soybean *GmGLP10* gene (Zhang et al. 2018). Rice overexpressing *OsGLP3-7* was also seen with enhanced levels of genes involved in jasmonic acid and phytoalexin biosynthesis pathways (Sun et al. 2023).

GLPs display diverse expression patterns, multiple biochemical activities, and critical roles in plant development and stress tolerance (Barman and Banerjee 2015; Liao et al. 2021; Yuan et al. 2021; Zaynab et al. 2022). In tomato, both biotic and abiotic stresses significantly impact growth and productivity, highlighting the potential role of GLP genes as valuable genetic resources for enhancing disease resistance and stress tolerance.

Material and methods:

Identification of the *SlGLP* Gene family in Tomato

For the genome-wide identification of tomato *SlGLP* gene family, GLP sequences from *Arabidopsis* and rice were used as queries in BLASTn and BLASTp searches against the Sol Genomics Network (https://solgenomics.net/) database to find homologous gene loci in tomato (Fernandez-Pozo et al. 2015). The genome and protein sequences of the identified tomato *SlGLPs* were then downloaded from Solgenomics database (https://solgenomics.net/) (Fernandez-Pozo et al. 2015). Genomic and protein sequences of GLPs in *Oryza sativa* and *Arabidopsis thaliana* were retrieved from the Rice Genome Annotation Project (RGAP, http://rice.uga.edu/) and the *Arabidopsis* Information Resource (TAIR, https://www.arabidopsis.org/) websites, respectively (Rhee et al. 2003; Kawahara et al. 2013; Li et al. 2016). Also, the keyword “germin-like” was used to search for gene loci entries corresponding to tomato in the Sol Genomics Network database (Fernandez-Pozo et al. 2015). To ensure accuracy, all the obtained putative GLP sequences were subjected to conserved motif

identification using the National Centre for Biotechnology Information-Conserved Domain Database (NCBI-CDD, https://www.ncbi.nlm.nih.gov/Structure/cdd/cdd.shtml) to verify the presence of the cupin_1 domain (Marchler-Bauer et al. 2015). The putative GLPs containing cupin_1 (PF00190) domain, a characteristic feature of GLPs, were classified as members of the GLP gene family and further validated using HMMER3 scan service (https://www.ebi.ac.uk/Tools/pfa/hmmer3_hmmscan/) provided by European Bioinformatics Institute (EBI) (Madeira et al. 2022). The gene IDs were listed in order according to their chromosomal coordinates as per the Sol Genomics Network, and the genes were named accordingly. The protein length, molecular weight and isoelectric point (pI) of the GLPs were calculated using ExPASy (https://web.expasy.org/compute_pi/) and their subcellular localizations were predicted using WoLF PSORT (https://wolfpsort.hgc.jp/) (Horton et al. 2007; Artimo et al. 2012). The complete list of identified *SlGLPs* and their characteristics is provided in Supplementary Table S1.

Multiple Sequence Alignment and Phylogenetic Tree Analysis:

To study the phylogenetic relationships between the GLPs of tomato and other plant species, the full- length protein sequences of GLPs from tomato, rice, *Arabidopsis* and potato were aligned using the Muscle algorithm of the MEGA 6.0 software (Tamura et al. 2013). The alignment was used to construct a phylogenetic tree using the neighbour-joining method with pairwise alignment and a maximum likelihood of 1000 bootstrap replicates set, and an intergeneric phylogenetic tree was built (Zaynab et al. 2022).

Motif and Gene Structure Analysis:

To investigate the conserved motifs of GLP members from tomato, the complete amino acid sequences of GLPs were analysed using the Multiple Em for Motif Elicitation (MEME) tool (https://meme-suite.org/meme/tools/meme) of the MEME Suite (Bailey et al. 2015). The maximum number of motifs was set to six. For gene structure mapping, the CDS and

corresponding genomic sequences of tomato GLP genes were subjected to analysis by NCBI splign tool to identify the positions of UTRs and introns (Kapustin et al. 2008) (https://www.ncbi.nlm.nih.gov/sutils/splign/splign.cgi?textpage=online&level=form).

Further, the Gene Structure Display Server (GSDS 2.0, http://gsds.gao-lab.org/) tool was deployed to construct the map. The coordinates of the exons as well as that of the cupin_1 domain in BED format were used as input parameters along with the intrageneric phylogenetic tree file data in the Newick format (Hu et al. 2015).

Chromosomal localization and cis-elements analysis

The data related to the chromosomal locations of the GLP genes was analysed using MapGene2Chrom (http://mg2c.iask.in/mg2c_v2.0/) to reconstruct the gene chromosome position map (Jiangtao et al. 2015). To identify cis-acting regulatory elements in the promoters of GLP genes, 2000 base pairs upstream of the coding DNA sequence (CDS) of biotic stress responsive *SlGLPs* were extracted from the Sol Genomics Network database. The upstream sequence was subsequently scanned using the PlantCARE (http://bioinformatics.psb.ugent.be/webtools/plantcare/html/) tool to analyse the presence of various cis-regulatory elements (CREs) (Lescot et al. 2002). Details of the selected cis elements for the promoter analysis are mentioned in the supplementary Table S2.

Tissue specific expressions of *SlGLPs*

Expression patterns of tomato *SlGLPs* genes in various tissues including root, stem, leaf, bud and flower were analysed using publicly available transcriptomic data (Li et al. 2020). A heat map was prepared to visualize the same.

Plant Material, Fungal Cultures and Treatments

Tomato (*Solanum lycopersicum* L.) var Moneymaker, which is susceptible to the fungal pathogens *Alternaria solani* (As) and *Fusarium oxysporum f.sp. lycopersici* (Fol) was used in

this study. Seeds of the tomato var. Moneymaker were sown in pots containing soil and coco peat. They were kept in a greenhouse with a temperature maintained at 24-28 °C and a day:night length ratio being around 1:1. and allowed to germinate. Similarly, seeds of *Nicotiana benthamiana* was sown for the further infiltration experiments. Three-week-old tomato plants were subjected to various phyto-hormone treatments and pathogen inoculations. Hormone treatments were given using aqueous solutions of 1mM salicylic acid (SA), 100 µM methyl jasmonic acid (JA) and 100µM abscisic acid (ABA). Leaflets were inoculated with 10 µl of 10^4 /ml conidial suspension of *A. solani* on either side of the midrib. 5×10^6 spores/ml spore suspension of Fol was inoculated by root dip method (Hussain et al. 2018). For phytohormone treated sampling 6 and 24 hours per inoculation were chosen. Leaf samples infected with *Alternaria* were collected at 3 days post-inoculation (dpi), whereas root tissues infected with Fol were harvested at 5 dpi. Tissues were immediately snap-frozen in liquid nitrogen and then stored at -80° C until further use.

Identification of pathogen responsive GLPs and their expression analysis

Publicly available transcriptomic datasets were analysed to identify pathogen-responsive *SlGLPs*, leading to the detection of fifteen *SlGLPs* associated with biotic stress. (Sade et al. 2015; Tan et al. 2015; Sarkar et al. 2017; Zhao et al. 2018). Primers were designed for each selected gene using NCBI Primer BLAST (https://www.ncbi.nlm.nih.gov/tools/primer-blast/) primer designing tool (Ye et al. 2012) and their expression analysis was done in response to various phytohormones treatments and pathogen challenge (Supplementary Table S3). Total RNA was extracted using the Spectrum™ Plant Total RNA Kit (Sigma-Aldrich) according to the manufacturer's instructions, treated with DNase I, checked for DNA contamination after PCR using elongation factor 1-alpha (*EF1α*) primers followed by agarose gel electrophoresis on 1.8% agarose gel and then finally converted to cDNA using the RevertAid First Strand cDNA Synthesis Kit (Thermo-Scientific) according to the protocols. cDNAs of phytohormone

treated samples of two time points were pooled together for further analysis. To validate and investigate the expression pattern of pathogen responsive *SlGLP* genes, qRT-PCR was performed. Gene expression analysis was performed using three biological replicates, each consisting of pooled samples from three plants. The elongation factor 1-alpha (*SlEF1α*) was chosen as a housekeeping gene. The relative gene expression levels of each target gene were calculated using the 2-ΔΔCt relative quantitative method (Schmittgen and Livak 2008).

Construction of overexpression vector and Agroinfiltration of *Nicotiana benthamiana* leaves

To investigate the functional role of a pathogen responsive GLP, *SlGLP11-1*, we constructed a vector for its overexpression. Full length coding sequence of *SlGLP11-1*(*Solyc11g006730*) was amplified by PCR using *SlGLP11-1* specific primers from Tomato leaf cDNA and introduced into *pAlpha2-NPT II-Ubq10-CCD-Ter10* vector using a *Bsa I* restriction site (using one step clone enzyme (Vazyme, China). Plasmid was sequenced and transformed into thermo-competent *A. tumefaciens* GV3101 cells by the freeze/thaw shock method. *Nicotiana benthamiana* plants were then infiltrated using *A. tumefaciens* GV3101 strain harbouring the binary vector *pAlpha2-SlGLP11-1* and sampled at 3 dpi (Senthil-Kumar and Mysore 2014). DNA was extracted followed by checking of transiently expressing *SlGLP11-1* by PCR. The transiently overexpressing leaves were then used for disease phenotyping. RNA was extracted followed by DNAse treatment and cDNA synthesis mentioned as above. Expression levels were confirmed by qRT- PCR. The plant leaves were then checked for disease pathogenicity using *Botrytis cinerea* with respect to mock plants. 1 x 10^6 spores of *Botrytis cinerea* were inoculated on samples infiltrated with *Agrobacterium* containing backbone vector (control) and *SlGLP11-1-OE* construct. Disease scoring and sampling was done after 3 days of inoculation. Disease severity was calculated in terms of Percentage Disease Index (PDI) (Roylawar et al. 2015).

Construction of a Virus-Induced Gene Silencing (VIGS) Vector and Agroinfiltration in *Solanum lycopersicum* Leaves

The coding sequence (CDS) of the gene of interest, *SlGLP11-1*, was PCR-amplified using gene-specific primers incorporating BamH1 restriction enzyme overhangs. The amplified product and the pTRV2 vector harbouring the magnesium chelatase (*SlMgche*) fragment were digested with the BamH1 at 37ºC. The digested PCR product was purified and ligated into the linearized pTRV2 vector using T4 DNA ligase. The ligation mixture was transformed into competent *Escherichia coli* cells, and transformed colonies were selected on antibiotic-containing medium. Positive colonies were initially screened by colony PCR using gene and backbone-specific primers to confirm the presence of the insert. The recombinant plasmid was sequenced, transformed, and agroinfiltrated following the procedures described above. Transient gene silencing in *Solanum lycopersicum* leaves was confirmed by quantitative RT-PCR (qRT-PCR) as outlined previously. Upon confirmation of silencing, leaves were subjected to pathogen infection assays using *Botrytis cinerea*. Mock-infiltrated plants served as controls, and disease progression was assessed as described above. Disease severity was quantified and compared between mock and transiently silenced leaves.

Estimation of Catalase Activity and Endogenous H_2O_2 Levels in Leaves Transiently Overexpressing and Silenced for *SlGLP11-1* gene

Catalase activity was assayed in agroinfiltrated *Solanum lycopersicum* leaves from control (EV), *SlGLP11-1*-overexpressing (*SlGLP11-1*OE), VIGS vector control (EV: TRV-*SlMgche*), and *SlGLP11-1*V (TRV-*SlMgche–SlGLP11-1*) samples, with and without pathogen inoculation. Approximately 100 mg of fresh leaf tissue was homogenized in 1 mL of ice-cold 0.1 M potassium phosphate buffer (pH 7.0) containing 5 µL Na-EDTA and 1% (w/v) polyvinylpyrrolidone (PVP). The homogenate was centrifuged at 14,000 rpm for 20 min, and

the supernatant was collected as the crude enzyme extract. Catalase activity was determined by monitoring the decomposition of H_2O_2 in a reaction mixture containing potassium phosphate buffer, 30 mM H_2O_2, and enzyme extract. The decrease in absorbance was recorded at 240 nm at 30 s intervals for 3 min, following the method of (Volk and Feierabend 1989). The mean change in absorbance per minute was used to calculate catalase activity, expressed as mKat mL^{-1} of enzyme extract.

Endogenous H_2O_2 levels were quantified in agroinfiltrated tomato leaves from control (EV), *SlGLP11-1*-overexpressing (*SlGLP11-1*OE), vector control for VIGS (EV: TRV-*SlMgche*), and *SlGLP11-1*V (TRV-*SlMgche–SlGLP11-1*) samples, with and without pathogen inoculation. Approximately 50 mg of leaf tissue was homogenized in 50 mM HEPES buffer. Three biological replicates were used, each comprising pooled samples from three leaves. Following centrifugation, the supernatant was collected as the crude extract. An aliquot of the extract was added to a reaction mixture containing 800 µL HEPES buffer, 1 µL H_2SO_4, and 100 µL potassium titanium oxalate. The absorbance was measured at 410 nm according to the method of Sellers (1980). Quantification of H_2O_2 was performed using a standard calibration curve generated with known concentrations of H_2O_2 (Kamble et al., 2013).

Results

Identification and Nomenclature of *SlGLP* Genes in Tomato Genome

A total of 29 distinct chromosomal loci encoding GLP genes were identified in tomato, in contrast to earlier reports that documented only 15 *SlGLP* genes. (Chattopadhyay, 2014). To maintain uniformity and avoid ambiguity, a new nomenclature for GLP family members in this study was proposed. The GLP genes were numbered according to their 1–11 chromosomal location and from top to bottom. Details of each GLP member, including the locus ID, protein length, and chromosomal location of all GLP genes are shown in the supplementary data Table 1. The *SlGLPs* genes encoded polypeptides with lengths ranging from 106 aa (*SlGLP1-1*) to

281 aa (*SlGLP9-4).* The molecular weight ranged from 11.73 kDa (*SlGLP1-1*) to 30.85 kDa (*SlGLP9-4*), and the pI values from 5.21 (*SlGLP9-1*) to 9.26 (*SlGLP11-1*). In silico subcellular localization prediction revealed localization of single *SlGLP,* each in the chloroplast, endoplasmic reticulum and plasma membrane. Two *SlGLPs* were located in the peroxisomes, three *SlGLPs* were located in the cytosol, six *SlGLPs* were located in the vacuole, and 15 *SlGLPs* were located in the extracellular region.

Phylogenetic Tree Analysis

To understand the phylogenetic relationships with in the *GLP* gene family, a total of 174 GLP protein sequences drawn four plant species including 29 from tomato (*Solanum lycopersicum; SlGLPs*), 70 from potato (*Solanum tubersum*; *StGLPs*), 43 from rice (Oryza sativa; *OsGLPs*) and 32 from *Arabidopsis thaliana*; *AtGLPs*) were used to conduct a comprehensive phylogenetic analysis. A neighbor-joining (NJ) phylogenetic tree was conducted using MEGA 6.0 with 1000 bootstrap replicates to ensure statistical robustness (Figure 1). According to the phylogenetic tree, all *GLP* proteins were distributed into six groups (groups I– VI). GLP members from the same chromosomal region consistently co-clustered with in same branch, reflecting the tandem duplication-driven organisation of GLP gene clusters. Groups I, III, IV and V were found to contain GLP members from all four species, suggesting that these clades represent ancestral lineages that diverged prior to the separation of monocots and dicots. In contrasts, Group II and VI were predominantly composed of tomato and potato GLP sequences comprising approximately 41% tomato and 59% potato GLPs, the largest of all six groups in terms of Solanaceae representation. The species restricted distribution suggests a lineage specific expansion of GLP genes within the solanaceae family. The preferential clustering of tomato and potato GLPs in these solanaceae exclusive clades indicates the closer evolutionary relatedness between these two species relative to their divergence from rice (monocotyledon)

and *Arabidopsis* (non-Solanaceae eudicot). Overall, these results reflects that while GLP gene

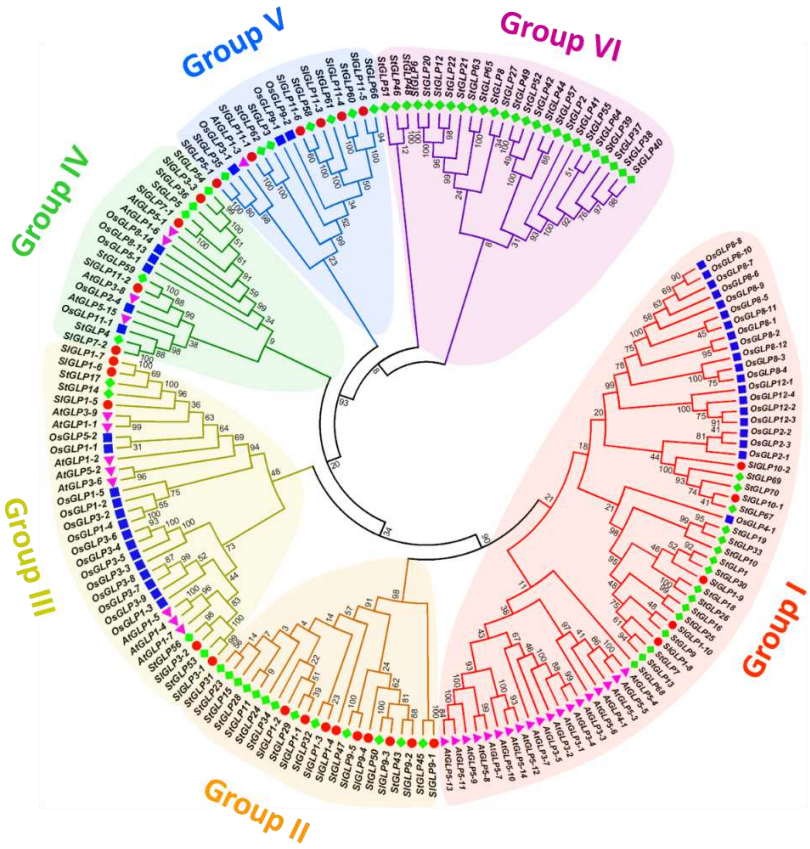


Fig. 1: Phylogenetic relationship of GLP proteins from *Arabidopsis* (32), Rice (43), *S. tuberosum* (70) and *S. lycopersicum* (29). The coloured shapes indicate different groups. The phylogenetic tree was generated using MEGA 6.0 with the NJ method with 1 000 bootstrap replicates. Group I, II, III, IV, V and VI are represented by pink, orange, yellow, green, blue and lavender colour respectively

family members share evolutionary origin across angiosperms, a subset of *SlGLP* genes underwent independent duplication and divergence specifically within Solanaceae lineage. This reflects functional specialization relevant to the specific biotic and abiotic challenges encountered by Solanaceae species.

Motif and Gene Structure Analysis

To investigate the structural diversity and evolutionary conservation of *SlGLP* proteins, conserved motif analysis was performed using MEME suite on the 29 tomato GLP amino acid sequences, resulting in the identification of six conserved motifs (Figure 2). Among them, motif

1 was present in all *SlGLPs* except for *SlGLP1-1*, and motif 2 and motif 3 also showed similar broad distribution. Notably, motif distribution patterns were largely congruent with phylogenetic grouping, suggesting that motif composition may reflect functional divergence among *SlGLP* subfamilies. Motif 4 displayed a group restricted distribution, occurring predominantly in *SlGLPs* belonging t group III and V, suggesting potential subfuntionalization within these clades. Conversely, Motif 5 was absent for most members of group III.

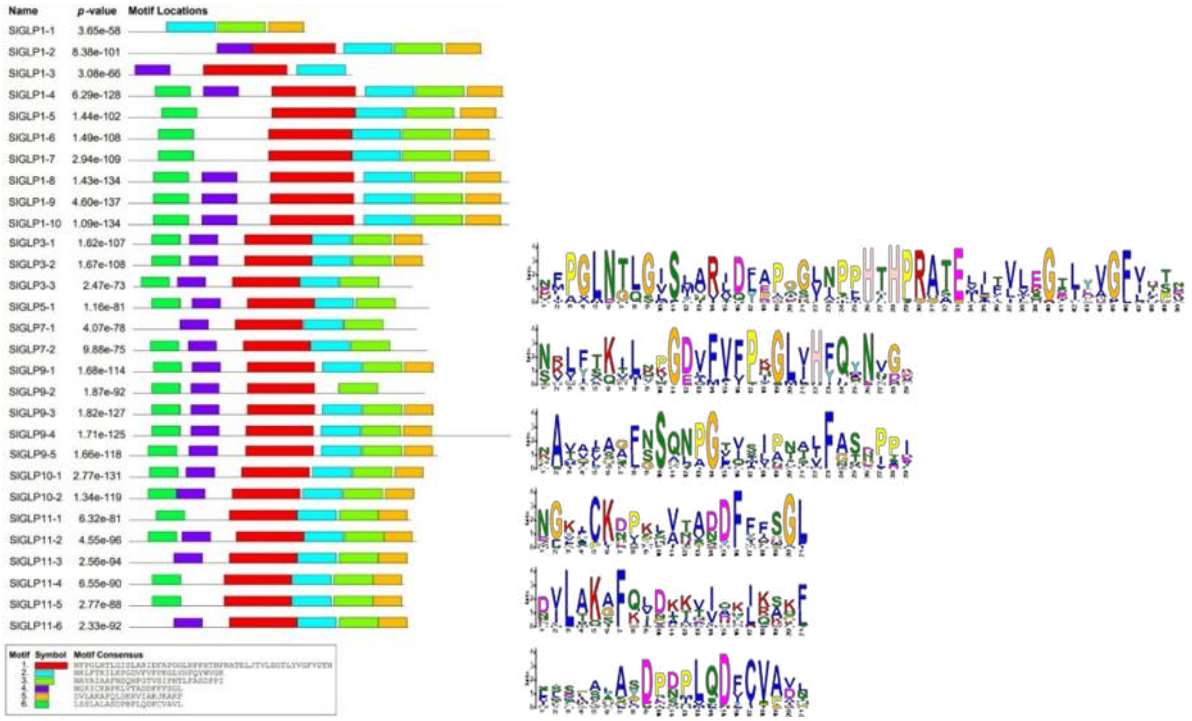


Fig. 2. Conserved motif distribution across 29 tomato (*Solanum lycopersicum*) GLP proteins as predicted by MEME analysis. Each horizontal bar represents a tomato GLP protein drown proportionally to its amino acid sequence length. Coloured boxes indicate the positions and relative lengths of six conserved motifs.

Diversity in gene structure mainly in the intron number and position is considered as an important mechanism underlying the functional divergence and evolutionary expansion of multigene families in plants. Analysis of the genomic organization of all 29 *SlGLP* genes using the Gene Structure Display Server (GSDS 2.0) revealed considerable structural heterogeneity (Figure 3). The intron number of the *SlGLP* genes ranged from 0 to 5, with the predominant

gene structure comprising two exons separated by a single intron, a configuration observed in 15 of 29 genes (51.7%). Interestingly, 11 *SlGLP* genes were found to be intron less, and these were concentrated within Group V, suggesting that intron loss may have contributed to the diversification of this clade. Conversely, *SlGLP9-2* and *SlGLP9-4* genes both member of Group II, harboured two introns.

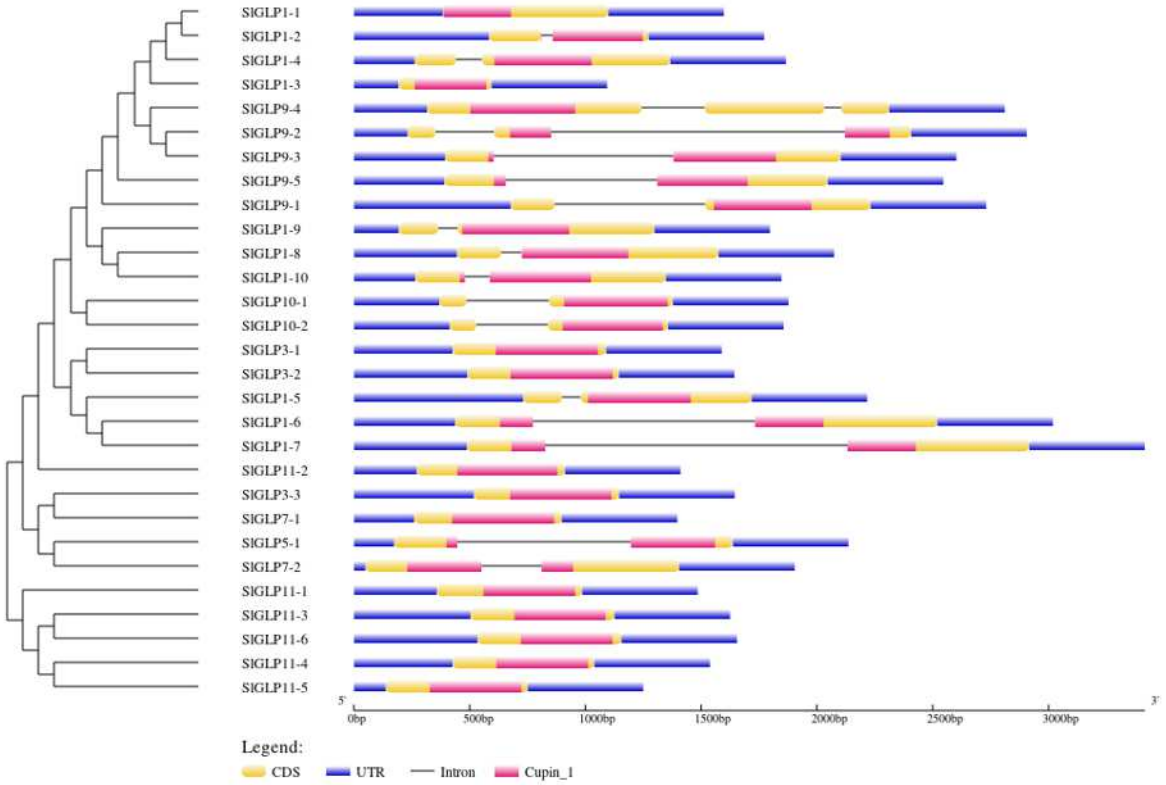


Fig. 3 Gene structure organization of 29 *Solanum lycopersicum* GLP (*SlGLP*) genes. Both 5' and 3' UTRs are represented by blue boxes, CDS are represented by yellow boxes and intron as black line. Pink box denotes the conserved Cupin 1 superfamily domain within the coding sequence. For each gene, the structural elements are drawn to scale relative to genomic sequence length (0-3000 bp; scale bar shown)

Chromosomal localization and cis-elements analysis

To determine the chromosomal locations of *SlGLP* genes within the tomato genome, the genomic coordinates of all 29 members were retrieved from the Sol genomics Network (SGN; genome assembly SL4.0) and mapped onto the 12 tomato chromosomes, with chromosome

2,4,6,8 and 12 harbouring no *SlGLP* loci (Figure 4). Chromosomal distribution analysis of *SlGLPs* depicted their unequal localization on all the chromosomes. Chromosome 1 contained the largest number of *SlGLP* genes (10/29), followed by chromosome 11 (6/29) and chromosome 5 (1 gene). The clustering of multiple *SlGLP* paralogs on the chromosomes 1,9, and 11 suggests that tandem duplication events may have contributed to the expansion of the *SlGLP* family on these chromosomes.

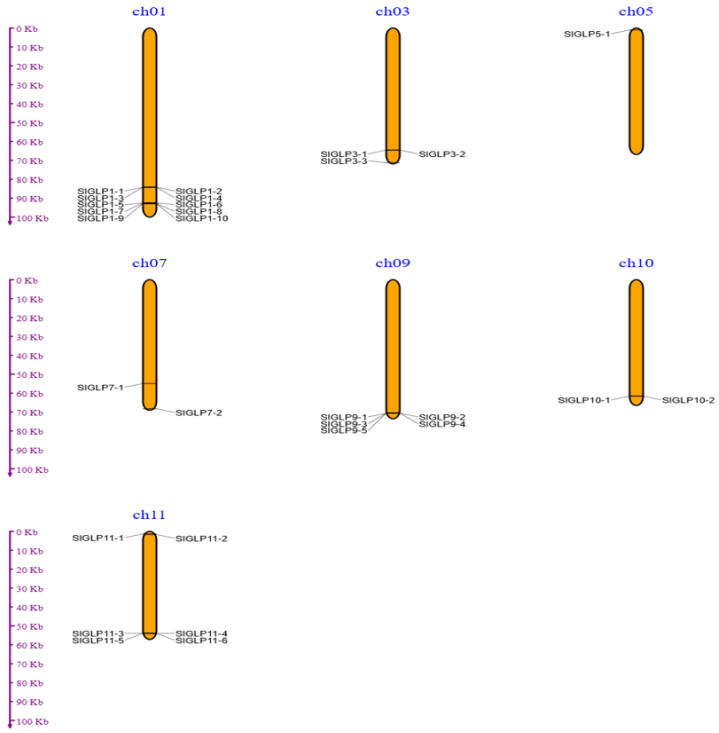


Fig. 4 Chromosomal localization of 29 *SlGLP* genes across tomato genome. Chromosome numbers are indicated above each ideogram. Black horizontal tick marks indicate the chromosomal positions of individual *SlGLP* genes with gene names labelled accordingly.

The precise genomic coordinates of each *SlGLP* gene are provided in Table 1.

To understand the potential regulatory mechanism governing the *SlGLP* gene expression, a 2000 bp upstream promoter region of each *SlGLP* gene was analyzed for the cis-regulatory elements (CREs) using the PlantCARE database (Figure 5). Multiple hormone- and stress-responsive CREs were identified, including elements associated with abscisic acid (ABREs),

jasmonic acid (CGTCA/TGACG), salicylic acid (TCA element). Gibberellin (GARE motif), and auxin (AuxRE) responsiveness suggesting the potential involvement of *SlGLP* genes in phytohormone mediated stress associated signaling pathways. Additionally, light responsive low temperature and anaerobic condition responsive cis elements were also observed. The presence of diverse biotic and abiotic stress associated CREs in *SlGLP* promoters collectively implies that these genes respond to a wide range of stress, consistent with the established roles of the GLPs protein in plant stress tolerance and defence.

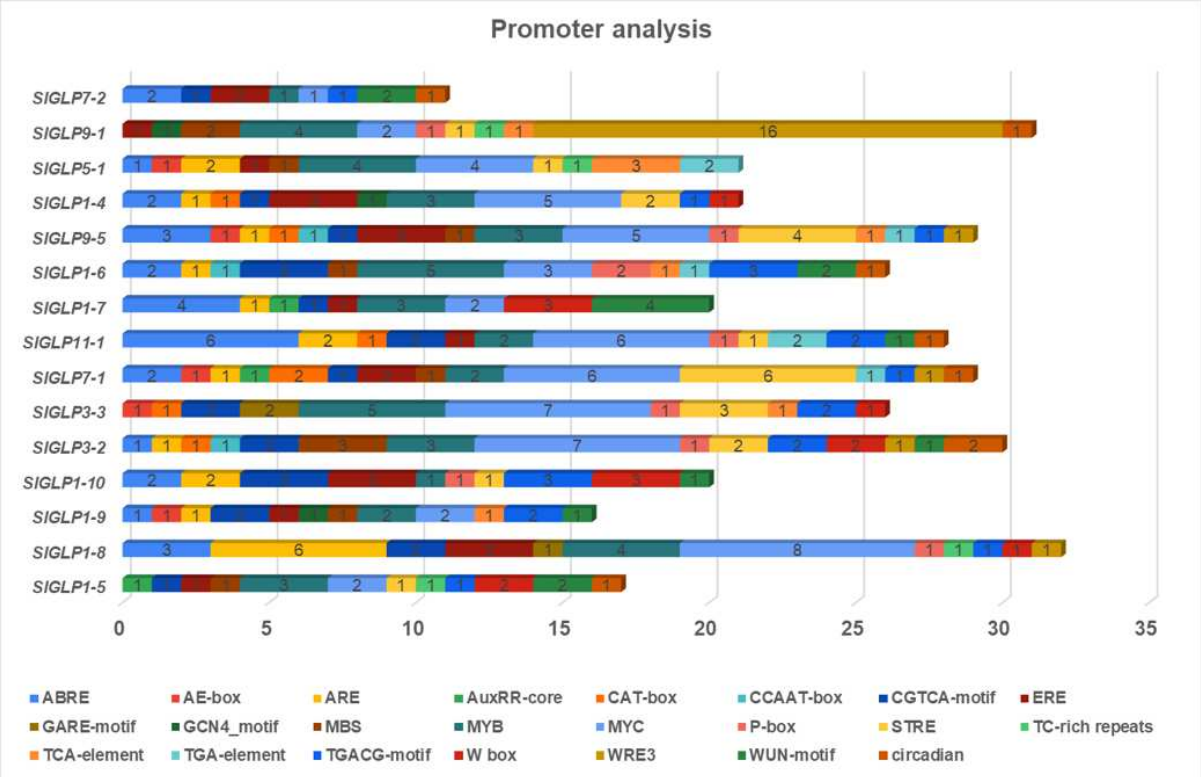


Fig. 5 Distribution and frequency of *cis*-regulating elements (CREs) in the 2000bp upstream promoter regions of pathogen responsive *SlGLP* genes

Tissue/organ specific expression of *SlGLPs*

To gain insight into the tissue- and developmental stage specific roles of *SlGLP* genes, their expression profiles across eight tomato tissue (root, stem, leaf, bud, flower, immature fruit,

mature fruit, and ripened fruit) were examined using RNAseq dataset (Li et al. 2020). The expression profiles revealed considerable diversity in tissue specificity, with *SlGLP* genes exhibiting constitutive, tissue preferential, or near absent expression patterns. *SlGLP7-1* displayed the highest overall expression level, with elevated TPM values in stem, leaf, and bud tissues suggesting a prominent role in vegetative development. *SlGLPs* like *SlGLP1-6, -1-7, -9-4* and *-9-5* exhibited broadly constitutive expression across all eight tissues examined, indicative of potential housekeeping, or multi-functional roles (Figure 6) . Conversely, nine *SlGLP* genes namely *SlGLP1-2, -1-3, -9-3*, *-10-1, -10-2, -11-1, -11-3, -11-4, -11-5* displayed consistently low or undetectable expression across all tissues, suggesting either highly condition specific induction or possible pseudogenization. Root preferential expression was also observed for *SlGLP1-5, -1-8, -1-9, -1-10, -3-1, -3-2, -5-1, -7-2, -9-1,* with *SlGLP1-9*

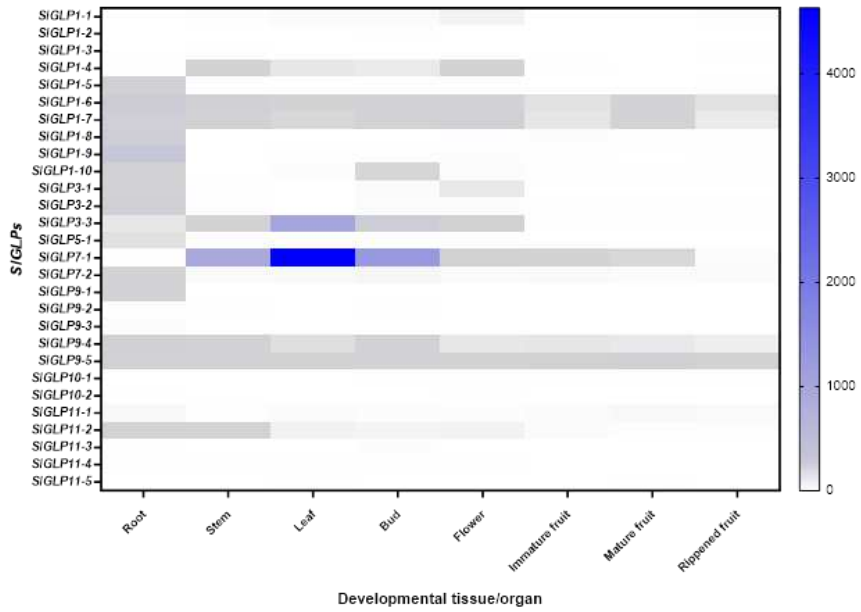


Fig. 6 Tissue and organ specific expression profiles of *SlGLP* genes in various tomato developmental stages. Color intensity ranges from white (low/absent expression) to deep blue (high expression). The expression heat map is created by taking normalized values of fragments Transcripts Per Million (TPM). The color scale bar is shown on the right.

recording the highest TPM among root expressed members implying their role in root growth and development. *SlGLP1-1*and *SlGLP9-5* showed expression in flower and fruit tissues respectively. Overall, the spatially distinct expression profile of *SlGLP* genes indicates functional diversification across developmental contexts, consistent with the known role of GLP family members in growth, defence, and stress responses in other plant species.

Expression profile of selected pathogen responsive *SlGLP* genes in response to SA, JA and ABA

Based on publicly available RNAseq datasets (Sade et al. 2015; Tan et al. 2015; Sarkar et al. 2017; Zhao et al. 2018). 15 *SlGLP* genes were identified which showed significant increase in the expression in response to diverse pathogens. Further, to get more insight, their expression was validated and examined in response to exogenous application of stress associated phytohormones including salicylic acid (SA), jasmonate (JA) and abscisic acid (ABA) (Figure 7a).

The majority of the 15 *SlGLP* genes showed statistically significant differential expression ($p<0.05$ or $p<0.01$) in response to at least one phytohormone treatment, indicating broad transcriptional responsiveness of the *SlGLP* family to phytohormone-mediated signaling. SA treatment induced the most pronounced upregulation in the largest number of *SlGLP* genes as compared to water treated control plants; *SlGLP1*-5 exhibited the highest SA-induced expression (~16,000-fold), followed by *SlGLP1-8* (~500-fold), *SlGLP1-9* (~20-fold), *SlGLP1-10* (~500-fold), *SlGLP3-3* (~7-fold), *SlGLP7-1* (~220-fold), and *SlGLP9-5* (~120-fold). In contrast, *SlGLP7-2, SlGLP9-1, SlGLP5-1, SlGLP1-4* and *SlGLP1-7* were significantly

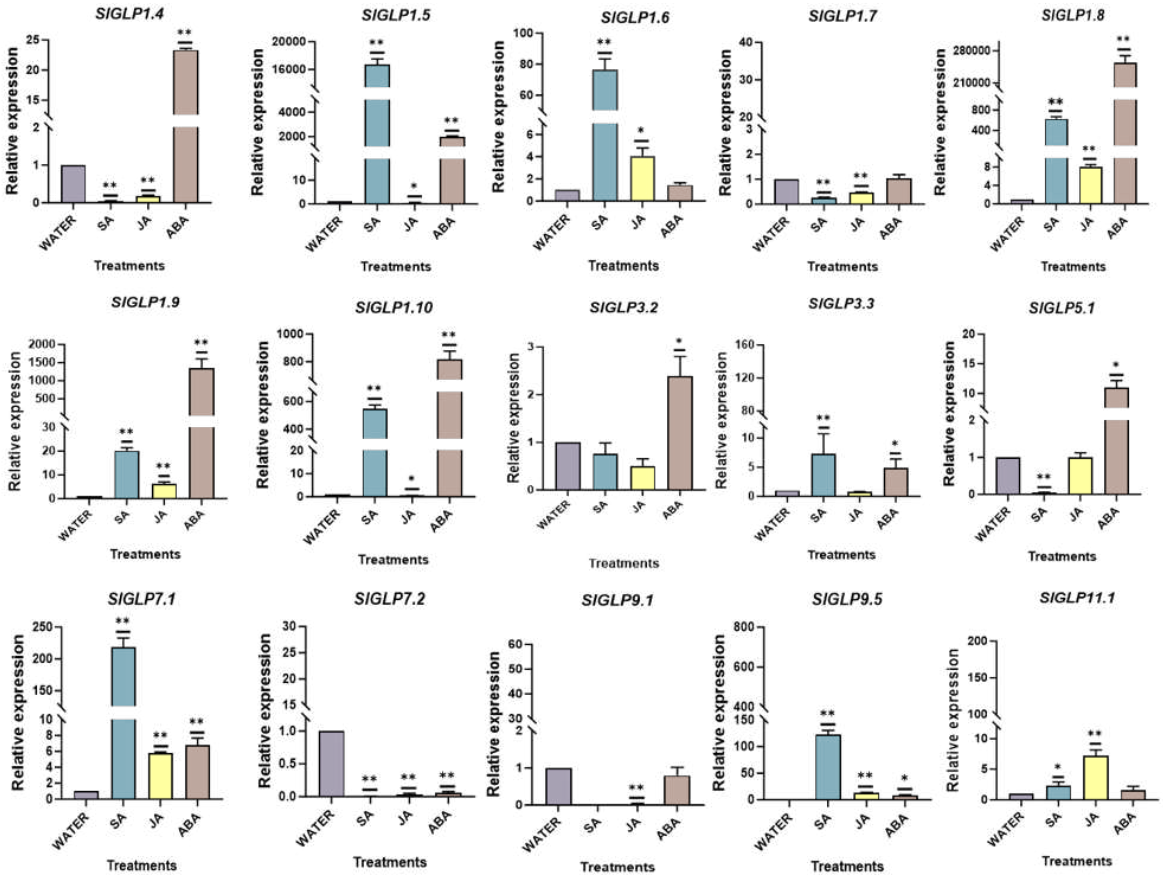


Fig.7 a Relative expression levels of pathogen responsive *SlGLP* genes in tomato leaf tissue in response to exogenous phytohormone treatments

The data are represented as the mean ±SD (n=3). The tomato *SlEFα* gene was used as an internal control. Asterisks indicate a significant difference ($p \leq 0.05$*; $p \leq 0.01$**) in expression between water and phytohormone treatments. SA: salicylic acid; JA: jasmonic acid; ABA: abscisic acid

downregulated by SA treatment, indicating gene-specific suppression under this pathway. ABA treatment induced the strongest overall upregulation for several members; *SlGLP1-8* showed the highest ABA-responsive expression (~250,000-fold), the largest fold-change recorded across all treatments and genes in this study, followed by *SlGLP1-9* (~1100-fold) and *SlGLP1-10* (~800-fold), indicating a prominent role for ABA-mediated signaling in regulating this subset of *SlGLP* genes, potentially linking them to abiotic stress responses. *SlGLP1-4* also

showed significant ABA-induced upregulation (~23-fold), while *SlGLP1-5* and *SlGLP1-6* exhibited moderate ABA responses (Figure 7a). JA treatment elicited a more selective response; *SlGLP1-6, SlGLP1-8, SlGLP1-9, SlGLP7-1* and *SlGLP11-1* showed significant increase in expression (~4-7-fold), while *SlGLP1-5* and *SlGLP9-5* showed a modest but significant increase. Several genes, including *SlGLP7-2, SlGLP9-1, SlGLP1-7, SlGLP1-4* and *SlGLP7-2*, were downregulated by JA treatment.

Notably, *SlGLP1-7* exhibited relatively stable expression across all three phytohormone treatments, suggesting constitutive activity or insensitivity to these hormonal inputs under the tested conditions. Taken together, the differential and largely significant expression responses of *SlGLP* genes to SA, JA, and ABA establish that multiple *SlGLP* family members are transcriptionally regulated by phytohormone signaling pathways associated with both biotic and abiotic stress responses in tomato.

Expression profile of selected pathogen responsive *SlGLP* genes in response to foliar necrotrophic pathogen *Alternaria solani*

A. solani inoculation induced highly significant ($p < 0.01$) and dramatic upregulation in a subset of *SlGLP* genes. The most striking response was observed for *SlGLP11-1*, which exhibited the highest induction (~2.5 × 10^6-fold relative to Mock), followed by *SlGLP1-9* which showed

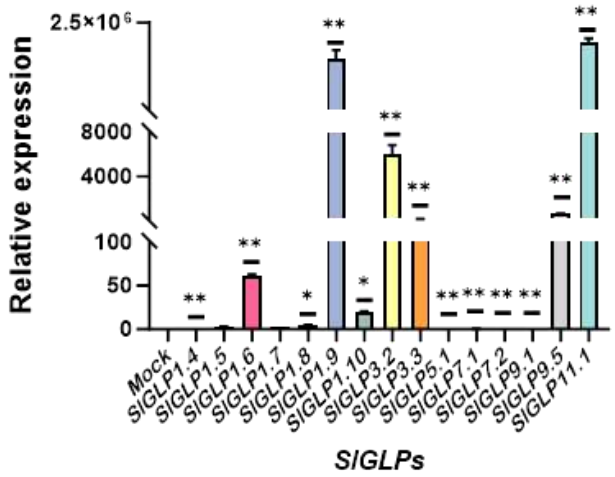


Fig.7b Relative expression levels of pathogen responsive *SlGLP* genes in tomato leaf tissue in response to *Alternaria solani* (As) inoculation

The data are represented as the mean ±SD (n=3). The tomato *SlEFα* gene was used as an internal control. Asterisks indicate a significant difference ($p \leq 0.05$*; $p \leq 0.01$**) in expression between mock: water inoculated and *Alternaria solani* inoculated leaves.

induction in the high-fold range (~10,000-fold and ~9,000-fold, respectively). *SlGLP3-2*, *SlGLP9-5* and *SlGLP3-3* were also robustly induced (~200-fold, 600-fold and ~4,500-fold, respectively) (Figure 7b). The exceptional magnitude of induction in these genes, particularly *SlGLP11-1 SlGLP1-9* and *SlGLP3-2* strongly implicates them as key transcriptional responders to *A. solani* infection, consistent with a role in early or amplified defence signaling against this necrotrophic pathogen. In contrast, several *SlGLP* genes including *SlGLP1-4*, *SlGLP1-5*, *SlGLP1-6*, *SlGLP1-10*, *SlGLP5-1*, *SlGLP7-1*, *SlGLP7-2*, and *SlGLP9-1* exhibited low but statistically significant ($p < 0.05$ or $p < 0.01$) responses to *A. solani* inoculation, with expression levels remaining near or only marginally above mock levels.

Expression profile of selected pathogen responsive *SlGLP* genes in response to vascular hemibiotrophic pathogen *Fusarium oxysporum f.sp. lycopersici*

FOL inoculation elicited significant and broad transcriptional induction across the majority of the 15 *SlGLP* genes examined in root tissue. *SlGLP9-1* exhibited the highest fold-induction (~50-fold; $p < 0.01$) relative to mock, followed by *SlGLP9-2* (~27-fold; $p < 0.01$) and *SlGLP7-*

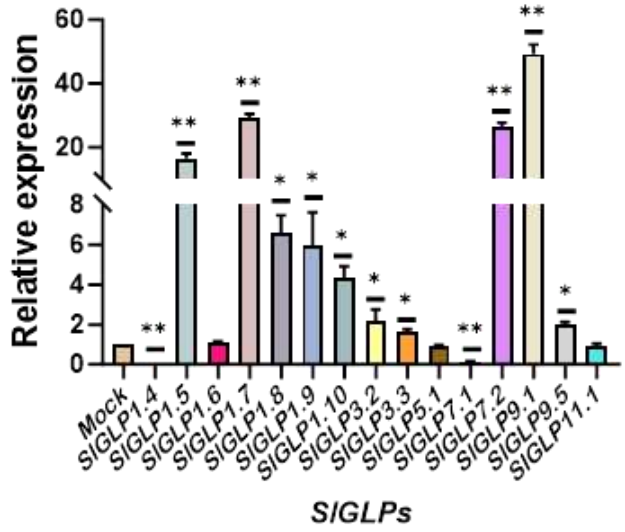


Fig.7c Relative expression levels of pathogen responsive *SlGLP* genes in tomato root tissue in response to *Fusarium oxysporum f. sp. lycopersici* (Fol) inoculation

Mock: water inoculated control root. The data are represented as the mean ±SD (n=3). The tomato *SlEFα* gene was used as an internal control. Asterisks indicate a significant difference ($p \leq 0.05$*; $p \leq 0.01$**) in expression between water and Fol inoculated roots.

2, *SlGLP1-7* (~25-fold; $p < 0.01$), identifying these three genes as the most robustly Fol-responsive *SlGLP* members (Figure 7c). Additional significantly upregulated genes included *SlGLP1-5* (18- fold), *SlGLP1-8* (~8-fold), *SlGLP1-9* (~7-fold), *SlGLP1-10* (~5-fold), *SlGLP3-2*, *SlGLP3-3* and *SlGLP5-1* (~1 to 2- fold) all significant at $p < 0.05$ or $p < 0.01$.

Functional characterization of a pathogen responsive *SlGLP11-1*

To investigate the functional role of *SlGLP11-1* in biotic stress responses, we established both gain-of-function and loss-of-function systems through agroinfiltration-based transient transformation. RT-qPCR analysis confirmed robust overexpression (OE) of *SlGLP11-1* in all five independently infiltrated *N. benthamiana* plants harbouring the *SlGLP11-1*OE construct (Figure 8).

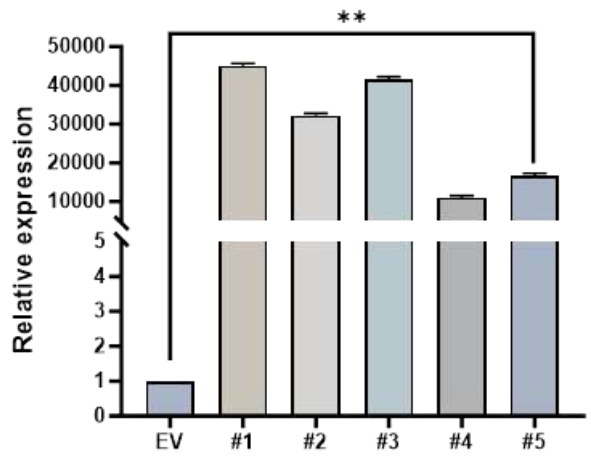


Fig.8. Confirmation of *SlGLP11-1* overexpression in transiently transformed *Nicotiana benthamiana* leaves. Relative transcript levels of *SlGLP11-1* in agroinfiltrated *Nicotiana* leaves transiently overexpressing *SlGLP11-1* as compared with the empty vector (EV) control post 72 hours of agroinfiltration. The data are represented as the mean +- SD (n=3). Asterisks indicate a significant difference ($p < 0.05$*; $p < 0.01$**) in expression between control and overexpressed plants. #1 to #5 denotes agroinfiltrated leaves of independent plants.

Relative transcript levels in OE lines ranged from approximately 10,000- to 44,000-fold as compared to the EV (Empty vector) control, with plants #1 and #3 showing the highest transcript accumulation. The difference between the OE lines and the EV control was statistically significant ($p < 0.01$), validating the efficacy of the overexpression system.

To evaluate the functional role of *SlGLP11-1* in resistance against the necrotrophic fungal pathogen *Botrytis cinerea*, a detached leaf bioassay was conducted on *N. benthamiana* leaves transiently expressing either the *SlGLP11-1* overexpression construct or the EV vector control. Scoring of disease at 3 days post-inoculation (dpi) revealed a striking contrast in severity of disease symptoms between the two treatments (Figure 10a). Leaves of EV-infiltrated plants developed large, rapidly spreading necrotic lesions that frequently covered a substantial proportion of the leaf surface, indicative of high susceptibility to *B. cinerea*. In contrast, *SlGLP11-1*OE leaves exhibited markedly restricted lesion development, with infection sites

remaining noticeably smaller and more contained, suggesting that elevated *SlGLP11-1* expression actively limits fungal colonization and tissue destruction.

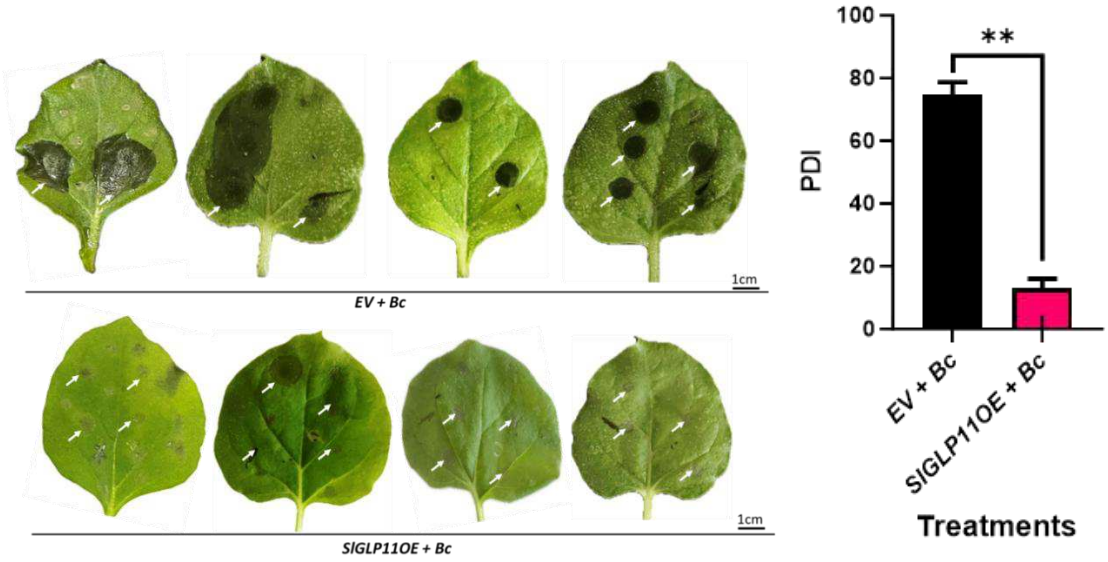


Fig.10. a) Agroinfiltrated detached leaves of *Nicotiana benthamiana* transiently overexpressing *SlGLP11-1* , 3 days after inoculation with a spore suspension of *B. cinerea* (1× 10^6 spores per ml). EV + *Bc*: *Botrytis cinerea* inoculated on leaf infiltered with *Agrobacterium* containing empty vector; OE + *Bc*: *Botrytis cinerea* inoculated on leaf infiltered with *Agrobacterium* harbouring *SlGLP11-1* overexpression vector. Error bars represent standard deviations (±SD). The experiment was repeated thrice with similar results.

b) Percent disease index (PDI) calculated using lesion diameters

Disease progress graph for *Botrytis cinerea* infection on *SlGLP11-1* transiently overexpressing *Nicotiana* plant leaves. Disease rate was measured, 3 days post inoculation by calculating the percentage of disease on 10 leaves/ treatment. Severity was scored for each leaf as the percentage of total leaf surface with symptoms (% lesion area), from 0 being free from infection to 5 being most severe with necrotic symptoms. Error bars represent standard deviations (±SD) of means. The experiment was repeated twice with similar results. Asterisks indicate a significant difference ($p < 0.05$*; $p < 0.01$**) in expression between mock and overexpressed plants.

Quantitative disease assessment by the Percent Disease Index (PDI) corroborated the phenotypic observations (Figure 10b). The EV + Bc control group had a mean PDI of approximately 75%, reflecting severe and widespread disease. In contrast, *SlGLP11-1*OE + Bc

leaves recorded a mean PDI of approximately 15%, representing an approximately 5-fold reduction in disease severity compared with the control. This difference was statistically significant ($p < 0.01$), and low variance among individual leaves in the OE treatment indicated a consistent and reproducible resistance phenotype. Taken together, these results demonstrate that transient overexpression of *SlGLP11-1* substantially enhances the resistance of *N. benthamiana* leaves to *B. cinerea*, strongly implicating this germin-like protein in the plant's defence response against necrotrophic pathogens.

Conversely, virus-induced gene silencing (VIGS) using the TRV-*SlMgche–SlGLP11*-1 construct resulted in a marked reduction of *SlGLP11-1* transcript levels in transiently silenced tomato leaves (Figure 9). All six silenced plants (#1–#6) showed substantially reduced expression relative to the TRV-*SlMgche* mock control, with relative transcript levels falling to

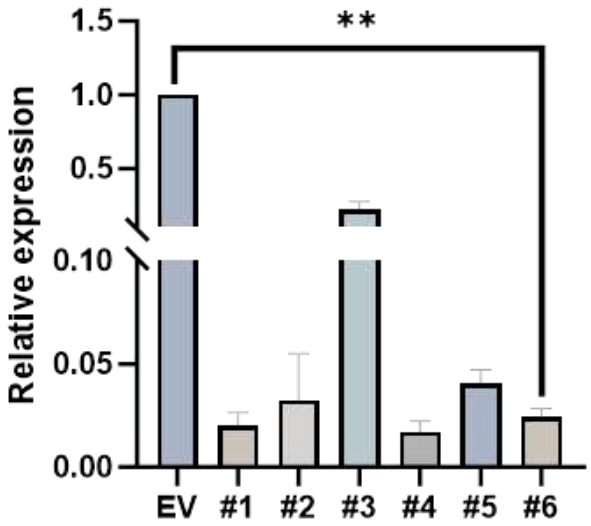


Fig.9. Confirmation of *SlGLP11-1* expression in Virus induced Gene Silenced (VIGS) *Solanum lycopersicum* Leaves

Relative transcript levels of *SlGLP11-1* in VIGS leaves of tomato leaves as compared with empty vector (EV) control plants at 72 h post-agroinfiltration. Data are presented as mean ± SD (n = 3 biological replicates). Asterisks indicate statistically significant differences in expression relative to the control ($p < 0.05$*; $p < 0.01$**). #1 to #5 denotes agroinfiltrated leaves of independent plants.

between approximately 2% and 9.5% of the control value. The degree of silencing was statistically significant ($p < 0.01$), although a degree of variability among individual lines was observed, as is typical for VIGS-based silencing. Taken together, these results confirm that the transient overexpression and silencing systems were both effective, providing a reliable experimental platform for subsequent functional analysis of *SlGLP11-1* in disease resistance.

To complement the overexpression data from *N. benthamiana* (Figure 10), we examined whether suppression of *SlGLP11-1* function in tomato was sufficient to compromise resistance against *B. cinerea*. VIGS-mediated silencing of *SlGLP11*-1 using the TRV-*SlMgche–SlGLP11*-1 construct led to a striking increase in disease severity compared with mock-infiltrated (TRV2MgChe) control leaves at 3 dpi (Figure 11a). Control leaves developed moderate, relatively contained lesions at inoculation sites, preserving much of the leaf tissue. In contrast, *SlGLP11*-1-silenced leaves displayed extensively spreading necrotic lesions accompanied by pronounced tissue chlorosis and collapse, consistent with a hyper susceptibility phenotype resulting from compromised basal defence.

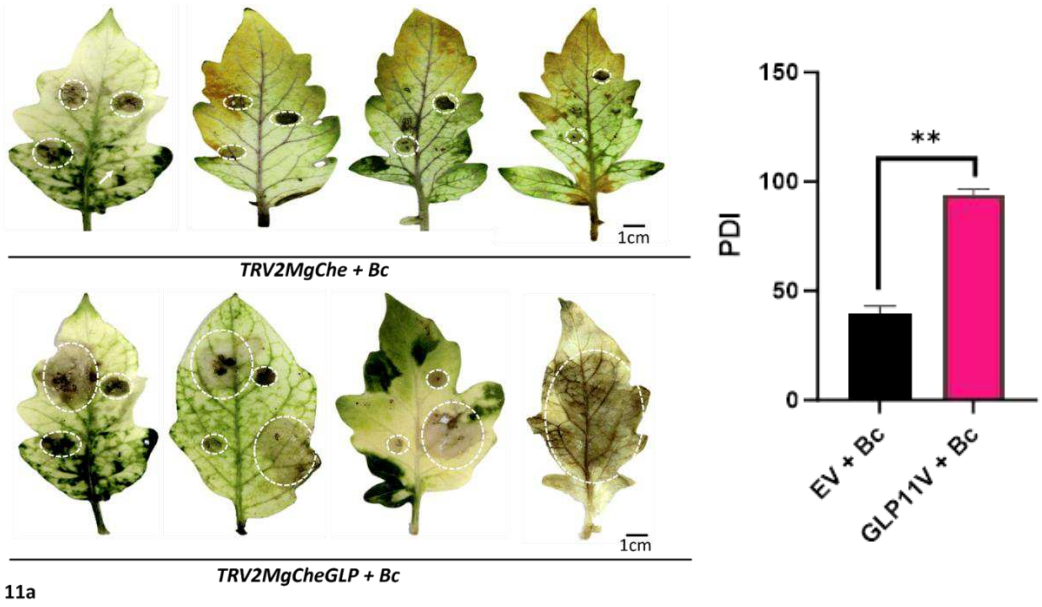


Fig.11. a) Detached leaves of control (Empty vector, EV- TRV-*SlMgche*) **and *GLP11* silenced (**TRV-*SlMgche–SlGLP11-1) **Nicotiana benthamiana* plants showing disease symptoms at 3 days after inoculation with a spore suspension of *B. cinerea* (1× 10^6 spores per ml). Lesion area shown in dotted line.** EV + *Bc* : *Botrytis cinerea* inoculated on leaf infiltered with *Agrobacterium* containing empty vector ; GLP11 + *Bc*: *Botrytis cinerea* inoculated on leaf infiltered with *Agrobacterium* containing TRV-*SlMgche–SlGLP11-1* silencing vetor. Error bars represent standard deviation (±SD). The experiment was repeated thrice with similar results.

b) Percent disease index (PDI) calculated using lesion diameters

Disease progress graph for *Botrytis cinerea* infection on tomato plants. Disease rate was measured, 3 days post inoculation by calculating the percentage of disease on 10 leaves/ treatment. Severity was scored for each leaf as the percentage of total leaf surface with symptoms (% lesion area), from 0 being free from infection to 5 being most severe with necrotic symptoms. Error bars represent standard deviations (±SD) of means. The experiment was repeated twice with similar results. Asterisks indicate a significant difference ($p < 0.05$*; $p < 0.01$**) in expression between mock and overexpressed plants.

Quantitative PDI analysis confirmed these phenotypic observations (Figure 11b). Mock-infiltrated control leaves (TRV2MgChe + Bc) had a mean PDI of approximately 40%, reflecting moderate but limited infection. By contrast, *SlGLP11-1*-silenced leaves (*TRV2MgCheGLP11* + Bc) recorded a mean PDI of approximately 95%, representing an approximately 2.4-fold increase in disease severity relative to the control, and this difference was statistically significant ($p < 0.01$). Individual leaf data points showed consistently high PDI

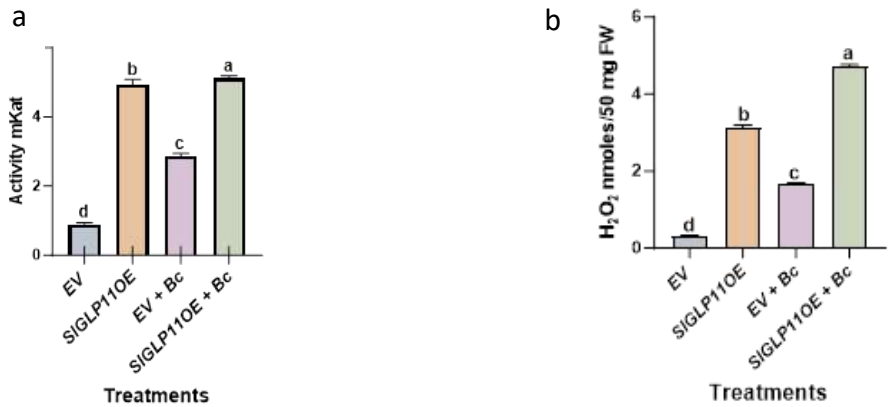
values in silenced plants with low variance, indicating a reproducible enhancement of susceptibility. Taken together with the overexpression results in Figure 10, these loss-of-function data provide reciprocal evidence that *SlGLP11-1* plays an active and necessary role in defence against the necrotrophic pathogen *B. cinerea* in tomato.

Estimation of endogenous H_2O_2 levels and catalase activity

To investigate the biochemical basis of *SlGLP11*-1-mediated resistance, endogenous H_2O_2 levels and catalase (CAT) activity were measured in both the overexpression (OE) and VIGS-silencing systems.

Overexpression of *SlGLP11*-1 potentiated the H_2O_2 accumulation in response to Botrytis challenge

Transient overexpression of *SlGLP11*-1 (*SlGLP11-1*OE) alone caused nearly 3-fold increase in H_2O_2 accumulation as compared to EV-infiltrated control leaves of *N. benthamiana* group and also significantly exceeding the level observed in EV plants inoculated with *B. cinerea* (EV + Bc) (Figure 12a). The highest H_2O_2 accumulation was observed in *SlGLP11-1*OE leaves subsequently challenged with *B. cinerea* (*SlGLP11-1*OE + Bc). These findings indicate that *SlGLP11-1* constitutively promotes H_2O_2 generation even in the absence of pathogen challenge, and that its effect is further potentiated after *B. cinerea* infection.



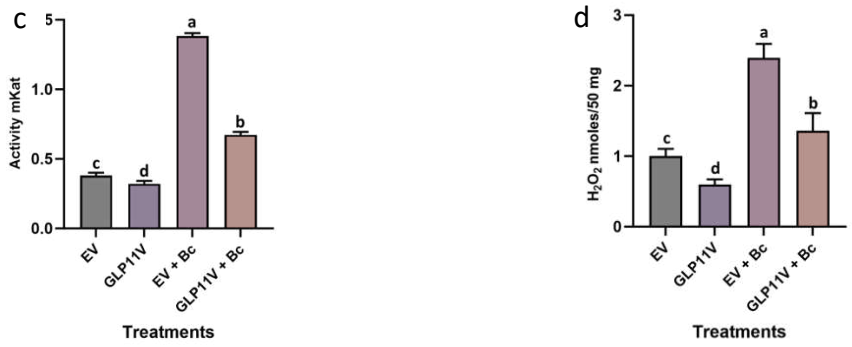


Fig.12 Endogenous H_2O_2 accumulation and catalase activity in *SlGLP11*-1 overexpressing (OE) and VIGS (V) silenced leaves with or without *Botrytis cinerea* challenge.

a Endogenous H_2O_2 levels in *N. benthamiana* leaves infiltrated with the empty vector (EV) control, the *SlGLP11-1* overexpression (*SlGLP11-1*OE), EV followed by *B. cinerea* inoculation (EV+Bc) and SlGLP11-1OE followed by *B. cinerea* inoculation (*SlGLP11-1*OE+Bc).

b Endogenous H_2O_2 levels in *S. lycopersicum* leaves infiltrated with the VIGS EV control (EV: *TRV2MgChe),* the *SlGLP11-1* silencing *TRV2MgCheGLP11* vector *(*GLP11V), EV followed by *B. cinerea* (EV+ Bc) and GLP11V followed by *B. cinerea* inoculation (GLP11V+Bc).

c Catalase activity in *N. benthamiana* leaves from the same OE treatments as described in (a)

d Catalase activity in *S. lycopersicum* leaves from the same VIGS treatments as described in (b)

Data points represent means of six independent samples, each representing the plant tissues pooled from five plants. Error bars represent standard deviations (±SD) of means. The experiment was repeated thrice with similar results. Within each set of experiments, the bars with different letters on the columns are significantly different at $P < 0.05$ according to Duncan's multiple test range (DMRT)

Silencing of *SlGLP11-1* resulted in reduced H_2O_2 accumulation

Silencing of *SlGLP11*-1 alone (GLP11V) reduced H_2O_2 below the basal level as observed in EV control plants, confirming that *SlGLP11-1* actively contributes to constitutive ROS homeostasis. Upon *B. cinerea* inoculation, mock-infiltrated control leaves mounted a robust oxidative burst producing the highest H_2O_2 (EV + Bc) (Figure 12b). Critically, silenced leaves challenged with the pathogen (GLP11V + Bc) showed a significantly attenuated H_2O_2 burst

compared to the infected control (EV+Bc). This ~42% reduction in H_2O_2 during infection in *SlGLP11-1*silenced plants directly mirrors the higher disease susceptibility observed

phenotypically (Figure 11), reinforcing the link between *SlGLP11-1* activity, ROS production, and resistance.

Catalase activity in the overexpression system

CAT activity in the OE system displayed a pattern that closely paralleled H_2O_2 levels, suggesting a co-regulatory relationship between ROS production and antioxidant scavenging capacity. EV controls showed the lowest CAT activity (Figure 12c). *SlGLP11-1*OE leaves without pathogen challenge showed a large increase in CAT activity and the highest CAT activity was recorded *in SlGLP11-1*OE + Bc leaves. EV + Bc plants showed an intermediate induction of CAT (Figure 12c).

Catalase activity in the silencing system

In the VIGS system, CAT activity aligned with the H_2O_2 pattern. Mock inoculated EV infiltrated control leaves displayed moderate basal CAT activity, while GLP11V-silenced mock inoculated leaves had the lowest activity, again consistent with reduced constitutive ROS levels. *B. cinerea* infection of mock-control leaves triggered the highest CAT induction, a response representing over a 3.5-fold increase above basal levels (Figure 12d).

However, in *SlGLP11-1*-silenced leaves challenged with the pathogen (GLP11V + Bc), CAT activity was significantly lower, ~51% reduction compared to infected controls. This suppressed CAT induction corresponds directly to the attenuated H_2O_2 burst in silenced-infected plants, confirming that less substrate (H_2O_2) is produced when *SlGLP11-1* is silenced, which in turn induces a proportionally weaker compensatory antioxidant response.

Discussion:

Tomato is exposed to different biotic and abiotic stresses and remains a key component of the global food chain making the identification of stress responsive gene families of direct agronomic relevance. Germin-like proteins (GLPs) are a functionally diverse protein family implicated in plant signalling and stress responses across the plant kingdom, with family size varying considerably between species, 32 *AtGLPs* in *Arabidopsis thaliana,* 43 *OsGLPs* in rice, 258 *TaGLPs* in wheat (Yuan et al., 2021) and 70 *StGLPs* in potato (Zaynab et al., 2022). In the present study, we provided an updated genome wide annotation and chromosome-based nomenclature for 29 *SlGLPs* in tomato (*Solanum lycopersicum*) nearly double the 15 members reported earlier (Chattopadhyay, 2014) with particular emphasis on the pathogen- responsive *SlGLPs* and their roles in plant immunity.

Structural analysis of the *SlGLP* family provides important clues to its functional organisation. Our findings highlight that the evolutionary trajectory of GLPs has been strongly influenced by exon–intron architecture. Consistent with previous reports, genes with short or absent introns tend to be preferentially retained in plant genomes during evolution, though they often exhibit relatively lower expression levels. In contrast, a compact gene structure may confer an adaptive advantage by facilitating rapid transcriptional responses of GLPs under diverse stimuli. Notably, the conserved exon–intron patterns observed across several *SlGLP* sequences, coupled with their shared functional properties, suggest that these genes likely originated through duplication events, reinforcing their evolutionary and functional significance in plants.

Cis-element analysis of *SlGLP* promoters identified motifs responsive to light, ABA, SA, GA, methyl jasmonate, low temperature, and anaerobic induction. The co-occurrence of these diverse elements within a 2 kb promoter window indicates that *SlGLPs* are placed under multi-hormonal and multi stimulus transcriptionally control. All identified *SlGLP* genes were

classified into six clades. Similar phylogenetic grouping was also observed in other plants. The comparative phylogenetic analysis revealed that the organization of *S. lycoperiscum*, *S. tuberosum*, and *A. thaliana* proteins was relatively similar in six clades, indicating that all *SlGLP* genes in these groups may have descended from a common ancestor. Previous studies reported the classification of GLPs into six clades in rice, *Arabidopsis* (Li et al., 2016) and in wheat and potato (Yuan et al., 2021; Zaynab et al., 2022).

Several previous studies have suggested that specific GLP family members play important roles in plant defence, making expression profiling of *SlGLPs* a valuable prerequisite for dissecting functional diversity within the family. GLPs have been reported to respond to phytohormones and abiotic stress in multiple species, consistent with their involvement in hormone-linked development and defence signalling. In this study, tomato leaves treated with SA, JA and ABA showed extensive significant differential expression of the fifteen candidates *SlGLPs*, confirming that these hormones actively engage the *SlGLP* transcriptional network. SA activated the broadest induction across the panel (mainly *SlGLP 1-5, SlGLP 1-8* and *SlGLP1-10*), ABA triggered the single largest fold induction notably *SlGLP1-8*, and JA induction was more selective but significant for several members, including *SlGLP11-1*. This pattern aligns with the already known fact regarding antagonism between SA associated defence against biotrophic/hemibiotrophic pathogens and JA associated defence against necrotrophs. SA/ABA responsive genes overlapped substantially with the genes induced by the hemibiotroph Fol, whereas the JA responsive *SlGLP11-1* showed its most dramatic induction upon infection with the necrotrophic *Alternaria* tested.

SlGLPs were upregulated following infection with the upon infection with the pathogenic fungi *A. solani* and Fol, confirming their involvement in biotic stress responses across pathogens with distinct infection strategies. Transient overexpression of the most strongly pathogen induced member *SlGLP11-1*, led to a substantial reduction in disease severity, providing direct

functional evidence for its role in tomato defence. The mean percent disease index (PDI) against *Botrytis cinerea* fell from approximately 75% in empty vector control leaves to approximately 15% in *SlGLP11-1* overexpressing leaves, a 5-fold reduction. While VIGS mediated silencing of *SlGLP11-1* produced the reciprocal outcome, raising mean PDI from approximately 40% in mock silenced controls to approximately 95% in silenced leaves. In wheat and Barley GLP4 imparted resistance to powdery mildew (Christensen et al., 2004; Zimmermann et al., 2006) and the cotton germin like protein *GhABP19*, directly inhibits growth of *B. cinerea* in vitro and its overexpression confers fungal resistance in planta (Pei et al. 2019).

GLPs are known to possess oxalate oxidase, SOD and catalase activities. These are recognised to catalyse harmful radicals into hydrogen peroxide, leading to increased levels of H_2O_2 (Woo et. 2000; Dunwell et al. 2008). In the present study, transient overexpression of *SlGLP11-1* alone in the absence of any pathogen challenge, increased H_2O_2 accumulation by nearly 3- fold relative to EV control leaves, and this basal elevation already exceeded the H_2O_2 level measured in EV control leaves that had been inoculated with *B. cinerea* (EV+Bc). This indicates that *SlGLP11-1* contributes directly and constitutively to apoplastic ROS generation, most likely through an oxalate oxidase or superoxide dismutase like enzymatic activity as reported for many other GLPs. Upon pathogen challenge, H_2O_2 levels increased further in all genotypes, but the increase was substantially amplified in *SlGLP11-1* overexpressing tissue, with *SlGLP11-1*OE+Bc leaves recording the highest H_2O_2 accumulation of any treatment combination in the study. This demonstrated that *SlGLP11-1* does not merely raise a static ROS baseline but actively potentiated the pathogen triggered oxidative burst, the magnitude of which corresponds closely to the near complete restriction of lesion development observed in the same overexpressing leaves.

The VIGS data provide the essential reciprocal confirmation. VIGS mediated silencing of *SlGLP11-1* reduced basal H_2O_2 below the level seen in mock silenced (EV) control leaves, directly demonstrating that *SlGLP11-1* contributes to constitutive ROS homeostasis even in uninfected tissue. Following *B. cinerea* inoculation, control leaves mounted a robust oxidative burst, but silenced leaves challenged with the pathogen showed a markedly attenuated response, with H_2O_2 leaves reduced by approximately 42% relative to infected controls. This reduced oxidative burst in *SlGLP11-1* silenced tissue correlates directly with the hypersusceptible phenotype (mean PDI nearly 95%). Taken together, the overexpression and silencing of *SlGLP11-1* positively and quantitively regulates the magnitude of the pathogen induced apoplastic oxidative burst, and the size of this burst is a strong predictor of resistance versus susceptibility to *B. cinerea*, consistent with the well-established roles of apoplastic H_2O_2 in direct antimicrobial activity, oxidative cross-linking and amplification of downstream defence signalling (Torres et al., 2006). In the overexpression system, EV control leaves showed the lowest CAT activity; *SlGLP11-1*OE leaves showed a significant increase in CAT activity even without pathogen challenge; EV+ Bc leaves showed an intermediate level of induction; and the highest CAT activity of all was recorded in *SlGLP11-1*OE leaves challenged with *B. cinerea*. In the VIGS system, the same but reverse trend was observed, EV control leaves showed moderate basal CAT activity that increased to its highest level following *B. cinerea* infection, whereas *SlGLP11-1* silenced leaves showed the lowest basal CAT activity and silenced leaves challenged with the pathogen showed a significant increase in CAT activity however remained lower than the EV control leaves challenged with pathogen. Overall, the results suggest that elevated *SlGLP11-1* activity drives a larger, potentiated H_2O_2 burst upon *B. cinerea* challenge, which is met by a proportionally scaled catalase based antioxidant response to maintain redox homeostasis, and the net outcome of this coordinate ROS production/scavenging system is markedly reduced lesion development and disease severity;

loss of *SlGLP11-1* function collapses this entire axis, lower basal and pathogen induced H_2O_2, weaker compensatory CAT induction, and corresponding higher susceptibility. In conclusion, this tight, quantitatively consistent relationship between *SlGLP11-1* dosage, oxidative burst magnitude, antioxidant response, and the PDI across two independent, reciprocal transient systems (Overexpression and VIGS) provides strong support for the role of *SlGLP11-1* in tomato immunity against necrotrophic pathogens.

Supplementary Data

All data generated this study are included in this published article [and its supplementary information file].

Data availability

All data supporting the findings of this study are available from the corresponding author upon reasonable request.

Conflict of interest

The authors declare that they have no conflict of interest.

References

Agarwal G, Rajavel M, Gopal B, Srinivasan N (2009) Structure-based phylogeny as a diagnostic for functional characterization of proteins with a cupin fold. PLoS One 4:e5736. https://doi.org/10.1371/journal.pone.0005736

Artimo P, Jonnalagedda M, Arnold K et al (2012) ExPASy: SIB bioinformatics resource portal. Nucleic Acids Res 40(W1):W597–W603. https://doi.org/10.1093/nar/gks400

Averyanov A (2009) Oxidative burst and plant disease resistance. Front Biosci (Elite Ed) 1:142–152. https://doi.org/10.2741/s14

Bailey TL, Johnson J, Grant CE, Noble WS (2015) The MEME Suite. Nucleic Acids Res 43(W1):W39–W49. https://doi.org/10.1093/nar/gkv416

Banerjee J, Maiti MK (2010) Functional role of rice germin-like protein1 in regulation of plant height and disease resistance. Biochem Biophys Res Commun 394:178–183. https://doi.org/10.1016/j.bbrc.2010.02.142

Barman AR, Banerjee J (2015) Versatility of germin-like proteins in their sequences, expressions, and functions. Funct Integr Genomics 15:533–548. https://doi.org/10.1007/s10142-015-0454-z

Beracochea VC, Almasia NI, Peluffo L et al (2015) Sunflower germin-like protein *HaGLP1* promotes ROS accumulation and enhances protection against fungal pathogens in transgenic *Arabidopsis thaliana*. Plant Cell Rep 34:1717–1733. https://doi.org/10.1007/s00299-015-1819-4

Bernier F, Berna A (2001) Germins and germin-like proteins: plant do-all proteins. But what do they do exactly? Plant Physiol Biochem 39:545–554. https://doi.org/10.1016/S0981-9428(01)01285-2

Carrillo MGC, Goodwin PH, Leach JE, Leung H, Vera Cruz CM (2009) Phylogenomic relationships of rice oxalate oxidases to the cupin superfamily and their association with disease resistance QTL. Rice 2:67–79. https://doi.org/10.1007/s12284-009-9024-0

Chattopadhyay T (2014) In silico analysis of the germin-like protein multigene family members of tomato with predicted oxalate oxidase activity. Int J Agric Environ Biotechnol 7:669–678.

Cheng X, Huang X, Liu S, Tang M, Hu W, Pan S (2014) Characterization of germin-like protein with polyphenol oxidase activity from *Satsuma mandarine*. Biochem Biophys Res Commun 449:313–318. https://doi.org/10.1016/j.bbrc.2014.05.027

Christensen AB, Thordal-Christensen H, Zimmermann G, Gjetting T, Lyngkjær MF, Dudler R, Schweizer P (2004) The germinlike protein GLP4 exhibits superoxide dismutase activity and is an important component of quantitative resistance in wheat and barley. Mol Plant Microbe Interact 17:109–117. https://doi.org/10.1094/MPMI.2004.17.1.109

Das A, Pramanik K, Sharma R, Gantait S, Banerjee J (2019) In-silico study of biotic and abiotic stress-related transcription factor binding sites in the promoter regions of rice germin-like protein genes. PLoS One 14:e0211887. https://doi.org/10.1371/journal.pone.0211887

Davidson RM, Reeves PA, Manosalva PM, Leach JE (2009) Germins: a diverse protein family important for crop improvement. Plant Sci 177:499–510. https://doi.org/10.1016/j.plantsci.2009.08.012

Dunwell JM, Gibbings JG, Mahmood T, Saqlan Naqvi SM (2008) Germin and germin-like proteins: evolution, structure, and function. Crit Rev Plant Sci 27:342–375. https://doi.org/10.1080/07352680802333938

Fernandez-Pozo N, Menda N, Edwards JD et al (2015) The Sol Genomics Network (SGN)—from genotype to phenotype to breeding. Nucleic Acids Res 43(D1):D1036–D1041. https://doi.org/10.1093/nar/gku1195

Godfrey D, Able AJ, Dry IB (2007) Induction of a grapevine germin-like protein (*VvGLP3*) gene is closely linked to the site of *Erysiphe necator* infection: a possible role in defence? Mol Plant Microbe Interact 20:1112–1125. https://doi.org/10.1094/MPMI-20-9-1112

Govindan G, KR S, Alphonse V, Somasundram S (2024) Role of germin-like proteins (GLPs) in biotic and abiotic stress responses in major crops: a review on plant defence mechanisms and stress tolerance. Plant Mol Biol Rep 42:450–468. https://doi.org/10.1007/s11105-024-01434-9

Ham BK, Li G, Kang BH, Zeng F, Lucas WJ (2012) Overexpression of *Arabidopsis* plasmodesmata germin-like proteins disrupts root growth and development. Plant Cell 24:3630–3648. https://doi.org/10.1105/tpc.112.101063

He ZD, Tao ML, Leung DWM et al (2021) The rice germin-like protein *OsGLP1* participates in acclimation to UV-B radiation. Plant Physiol 186:1254–1268. https://doi.org/10.1093/plphys/kiab125

Himmelbach A, Liu L, Zierold U et al (2010) Promoters of the barley germin-like GER4 gene cluster enable strong transgene expression in response to pathogen attack. Plant Cell 22:937–952. https://doi.org/10.1105/tpc.109.067934

Horton P, Park KJ, Obayashi T et al (2007) WoLF PSORT: protein localization predictor. Nucleic Acids Res 35(W2):W585–W587. https://doi.org/10.1093/nar/gkm259

Houde M, Diallo AO (2008) Identification of genes and pathways associated with aluminum stress and tolerance using transcriptome profiling of wheat near-isogenic lines. BMC Genomics 9:400. https://doi.org/10.1186/1471-2164-9-400

Hu B, Jin J, Guo AY, Zhang H, Luo J, Gao G (2015) GSDS 2.0: an upgraded gene features visualization server. Bioinformatics 31:1296–1297. https://doi.org/10.1093/bioinformatics/btu817

Huang N, Cheng X, Hu W, Pan S (2015) Inactivation, aggregation, secondary and tertiary structural changes of germin-like protein in *Satsuma mandarine* with high polyphenol oxidase activity induced by ultrasonic processing. Biophys Chem 197:18–24. https://doi.org/10.1016/j.bpc.2014.12.001

Hussain K, Mungikar K, Kulkarni A, Kamble A (2018) Identification, characterization and expression analysis of pigeon pea miRNAs in response to *Fusarium* wilt. Gene 653:57–64. https://doi.org/10.1016/j.gene.2018.02.017

Jiangtao C, Yingzhen K, Qian W et al (2015) MapGene2Chrom, a tool to draw gene physical map based on Perl and SVG languages. Hereditas 37:91–97. https://doi.org/10.16288/j.yczz.2015.01.013

Kamble A, Koopmann B, Von Tiedemann A (2013) Induced resistance to *Verticillium longisporum* in *Brassica napus* by β-aminobutyric acid. Plant Pathol 62:552–561. https://doi.org/10.1111/j.1365-3059.2012.02669.x

Kapustin Y, Souvorov A, Tatusova T, Lipman D (2008) Splign: algorithms for computing spliced alignments with identification of paralogs. Biol Direct 3:20. https://doi.org/10.1186/1745-6150-3-20

Kawahara Y, de la Bastide M, Hamilton JP et al (2013) Improvement of the *Oryza sativa* Nipponbare reference genome using next generation sequence and optical map data. Rice 6:4. https://doi.org/10.1186/1939-8433-6-4

Knecht K, Seyffarth M, Desel C et al (2010) Expression of BvGLP-1 encoding a germin-like protein from sugar beet in *Arabidopsis thaliana* leads to resistance against phytopathogenic fungi. Mol Plant Microbe Interact 23:446–457. https://doi.org/10.1094/MPMI-23-4-0446

Kurtz DM (2001) Germin is a manganese-containing homohexamer with oxalate oxidase and superoxide dismutase activities. Chemtracts 14:461–465.

Lane BG (2002) Oxalate, germins, and higher-plant pathogens. Funct Plant Biol 29:67–75. https://doi.org/10.1071/PP01078

Lescot M, Déhais P, Thijs G et al (2002) PlantCARE, a database of plant cis-acting regulatory elements and a portal to tools for in silico analysis of promoter sequences. Nucleic Acids Res 30:325–327. https://doi.org/10.1093/nar/30.1.325

Li L, Xu X, Chen C, Shen Z (2016) Genome-wide characterization and expression analysis of the germin-like protein family in rice and *Arabidopsis*. Int J Mol Sci 17:1622. https://doi.org/10.3390/ijms17101622

Li Y, Chen Y, Zhou L et al (2020) MicroTom Metabolic Network: rewiring tomato metabolic regulatory network throughout the growth cycle. Mol Plant 13:1203–1218. https://doi.org/10.1016/j.molp.2020.06.005

Liao L, Hu Z, Liu S, Yang Y, Zhou Y (2021) Characterization of germin-like proteins (GLPs) and their expression in response to abiotic and biotic stresses in cucumber. Horticulturae 7:412. https://doi.org/10.3390/horticulturae7100412

Liu H, Liu J, Wei Y (2016) Identification and analysis of the metacaspase gene family in tomato. Biochem Biophys Res Commun 479:523–529. https://doi.org/10.1016/j.bbrc.2016.09.103

Madeira F, Pearce M, Tivey ARN et al (2022) Search and sequence analysis tools services from EMBL-EBI in 2022. Nucleic Acids Res 50(W1):W276–W279. https://doi.org/10.1093/nar/gkac240

Manosalva PM, Davidson RM, Liu B et al (2009) A germin-like protein gene family functions as a complex quantitative trait locus conferring broad-spectrum disease resistance in rice. Plant Physiol 149:286–296. https://doi.org/10.1104/pp.108.128348

Marchler-Bauer A, Derbyshire MK, Gonzales NR et al (2015) CDD: NCBI's conserved domain database. Nucleic Acids Res 43(D1):D222–D226. https://doi.org/10.1093/nar/gku1221

Mejía-Teniente L, Joaquin-Ramos AJ, Torres-Pacheco I et al (2015) Silencing of a germin-like protein gene (*CchGLP*) in geminivirus-resistant pepper (*Capsicum chinense* Jacq.) BG-3821 increases susceptibility to infections by geminiviruses. Viruses 7:6141–6151. https://doi.org/10.3390/v7122930

Nakata M, Watanabe Y, Sakurai Y et al (2004) Germin-like protein gene family of a moss, *Physcomitrella patens*, phylogenetically falls into two characteristic new clades. Plant Mol Biol 56:381–395. https://doi.org/10.1007/s11103-004-3475-x

Osama R, Ogilvie CE, Fisher SR et al (2025) Transcriptional response to *Phytophthora* root rot in raspberry identifies *RiABP19*, a germin-like protein (GLP) gene with a putative role in resistance. bioRxiv [Preprint]. https://doi.org/10.1101/2025.07.07.663483

Patnaik D, Khurana P (2001) Germins and germin like proteins: an overview. Indian Journal of Experimental Biology, 39(3):191-200.

Pei Y, Li X, Zhu Y, Ge X, Sun Y, Liu N, Jia Y, Li F, Hou Y (2019) *GhABP19*, a novel germin-like protein from *Gossypium hirsutum*, plays an important role in the regulation of resistance to *Verticillium* and *Fusarium* wilt pathogens. Front Plant Sci 10:583. https://doi.org/10.3389/fpls.2019.00583

Pei Y, Zhu Y, Jia Y et al (2020) Molecular evidence for the involvement of cotton *GhGLP2* in enhanced resistance to *Verticillium* and *Fusarium* wilts and oxidative stress. Sci Rep 10:12510. https://doi.org/10.1038/s41598-020-68943-x

Perveen S, Khan TA, Shaheen H et al (2021) Morpho-physiological investigations in transgenic tomato (*Solanum lycopersicum* L.) overexpressing *OsRGLP1* gene. In Vitro Cell Dev Biol Plant 57:907–922. https://doi.org/10.1007/s11627-021-10165-5

Rhee SY, Beavis W, Berardini TZ et al (2003) The *Arabidopsis* Information Resource (TAIR): a model organism database providing a centralized, curated gateway to *Arabidopsis* biology. Nucleic Acids Res 31:224–228. https://doi.org/10.1093/nar/gkg076

Rietz S, Bernsdorff FEM, Cai D (2012) Members of the germin-like protein family in Brassica napus are candidates for the initiation of an oxidative burst that impedes pathogenesis of *Sclerotinia sclerotiorum*. J Exp Bot 63:5507–5519. https://doi.org/10.1093/jxb/ers203

Rodríguez-López M, Baroja-Fernández E, Zandueta-Criado A et al (2001) Two isoforms of a nucleotide-sugar pyrophosphatase/phosphodiesterase from barley leaves (*Hordeum vulgare* L.) are distinct oligomers of *HvGLP1*, a germin-like protein. FEBS Lett 490:44–48. https://doi.org/10.1016/S0014-5793(01)02135-4

Roylawar P, Panda S, Kamble A (2015) Comparative analysis of BABA and *Piriformospora indica* mediated priming of defence-related genes in tomato against early blight. Physiol Mol Plant Pathol 91:88–95. https://doi.org/10.1016/j.pmpp.2015.06.004

Sade D, Shriki O, Cuadros-Inostroza A et al (2015) Comparative metabolomics and transcriptomics of plant response to Tomato yellow leaf curl virus infection in resistant and susceptible tomato cultivars. Metabolomics 11:81–97. https://doi.org/10.1007/s11306-014-0670-x

Sakamoto A, Nishimura T, Miyaki Y-I, Watanabe S, Takagi H, Izumi S, Shimada H (2015) In vitro and in vivo evidence for oxalate oxidase activity of a germin-like protein from azalea. Biochem Biophys Res Commun 458:536–542.

Sarkar D, Maji RK, Dey S et al (2017) Integrated miRNA and mRNA expression profiling reveals the response regulators of a susceptible tomato cultivar to early blight disease. DNA Res 24:235–250. https://doi.org/10.1093/dnares/dsx003

Schmittgen TD, Livak KJ (2008) Analyzing real-time PCR data by the comparative CT method. Nat Protoc 3:1101–1108. https://doi.org/10.1038/nprot.2008.73

Schweizer P, Christoffel A, Dudler R (1999) Transient expression of members of the germin-like gene family in epidermal cells of wheat confers disease resistance. Plant J 20:541–552. https://doi.org/10.1046/j.1365-313X.1999.00624.x

Segarra CI, Casalongué CA, Pinedo ML, Ronchi VP, Conde RD (2003) A germin-like protein of wheat leaf apoplast inhibits serine proteases. J Exp Bot 54:1335–1341. https://doi.org/10.1093/jxb/erg139

Sellers RM (1980) Spectrophotometric determination of hydrogen peroxide using potassium titanium(IV) oxalate. Analyst 105:950–954. https://doi.org/10.1039/AN9800500950

Senthil-Kumar M, Mysore KS (2014) Tobacco rattle virus-based virus-induced gene silencing in *Nicotiana benthamiana*. Nat Protoc 9:1549–1562. https://doi.org/10.1038/nprot.2014.092

Shahwar D, Deeba F, Hussain I et al (2023) Characterization of the active site of a germin-like protein 1 as an oxidative stress defence enzyme in plants. Plant Gene 36:100432. https://doi.org/10.1016/j.plgene.2023.100432

Sultana T, Deeba F, Naz F, Rose RJ, Saqlan Naqvi SM (2016) Expression of a rice GLP in *Medicago truncatula* exerting pleiotropic effects on resistance against *Fusarium oxysporum* through enhancing FeSOD-like activity. Acta Physiol Plant 38:2273. https://doi.org/10.1007/s11738-016-2273-9

Sun B, Li W, Ma Y et al (2023) OsGLP3-7 positively regulates rice immune response by activating hydrogen peroxide, jasmonic acid, and phytoalexin metabolic pathways. Mol Plant Pathol 24:248–261. https://doi.org/10.1111/mpp.13294

Tamura K, Stecher G, Peterson D, Filipski A, Kumar S (2013) MEGA6: molecular evolutionary genetics analysis version 6.0. Mol Biol Evol 30:2725–2729. https://doi.org/10.1093/molbev/mst197

Tan G, Liu K, Kang J et al (2015) Transcriptome analysis of the compatible interaction of tomato with *Verticillium dahliae* using RNA-sequencing. Front Plant Sci 6:428. https://doi.org/10.3389/fpls.2015.00428

Torres MA, Jones JDG, Dangl JL (2006) Reactive oxygen species signaling in response to pathogens. Plant Physiol 141:373–378. https://doi.org/10.1104/pp.106.079467

Volk S, Feierabend J (1989) Photoinactivation of catalase at low temperature and its relevance to photosynthetic and peroxide metabolism in leaves. Plant Cell Environ 12:701–712. https://doi.org/10.1111/j.1365-3040.1989.tb01630.x

Wang T, Chen X, Zhu F et al (2013) Overexpression of rice germin-like protein *OsGLP2-1* enhances resistance to *Magnaporthe oryzae* and *Rhizoctonia solani* in transgenic rice. Plant Cell Rep 32:935–945. https://doi.org/10.1007/s00299-013-1420-7

Woo EJ, Dunwell JM, Goodenough PW, Marvier AC, Pickersgill RW (2000) Germin is a manganese-containing homohexamer with oxalate oxidase and superoxide dismutase activities. Nat Struct Mol Biol 7:1036–1040. https://doi.org/10.1038/80954

Ye J, Coulouris G, Zaretskaya I et al (2012) Primer-BLAST: A tool to design target-specific primers for polymerase chain reaction. BMC Bioinformatics 13, 134.

Yuan B, Yang Y, Fan P et al (2021) Genome-wide identification and characterization of germin and germin-like proteins (GLPs) and their response under powdery mildew stress in wheat (*Triticum aestivum* L.). Plant Mol Biol Rep 39:821–832. https://doi.org/10.1007/s11105-021-01291-w

Yuan Y, Xing H, Zeng W et al (2021) Genome-wide identification and characterization of germin and germin-like proteins in peanut (*Arachis hypogaea* L.). Int J Mol Sci 22:2305. https://doi.org/10.3390/ijms22052305

Zaynab M, Peng J, Sharif Y, Fatima M, Albaqami M, Al-Yahyai R, Khan KA et al (2022) Genome-wide identification and expression profiling of germin-like proteins reveal their role in regulating abiotic stress response in potato. Front Plant Sci 12:831140. https://doi.org/10.3389/fpls.2021.831140

Zhang N, Guan R, Yang Y et al (2017) Isolation and characterization of a *Fusarium oxysporum*-resistant gene *LrGLP1* from *Lilium regale* Wilson. In Vitro Cell. Dev. Biol.-Plant 53, 461–468.

Zhang Z, Ren C, Zou L et al (2018) Characterization of the germin-like protein (GLP) gene family in *Sesamum indicum* and their expression under stress and hormone treatments. BMC Genomics 19:1–13. https://doi.org/10.1186/s12864-018-4954-2

Zhao M, Ji M, Gao Y, Cao X, Mao Y, Ouyang Q, and Liu P (2018) An integrated analysis of mRNA and sRNA transcriptional profiles in tomato root: Insights on tomato wilt disease. PLoS ONE, 13(11): e0206765.

Zimmermann G, Bäumlein H, Mock HP, Himmelbach A, Schweizer P (2006) The multigene family encoding germin-like proteins of barley: regulation and function in basal host resistance. Plant Physiol 142:181–192. https://doi.org/10.1104/pp.106.083824

Supplementary Files

This is a list of supplementary files associated with this preprint. Click to download.

- SuppIdataGLP.docx